Science of the Total Environment 849 (2022) 157828

Contents lists available at ScienceDirect

Science of the Total Environment

journal homepage: www.elsevier.com/locate/scitotenv

Durability assessment of external thermal insulation composite systems in urban and maritime environments

J.L. Parracha [a,b,*], G. Borsoi [a,b], R. Veiga [a], I. Flores-Colen [b], L. Nunes [a,c], C.A. Viegas [d,e], L.M. Moreira [d,e], A. Dionísio [f], M. Glória Gomes [b], P. Faria [g]

[a] LNEC, National Laboratory for Civil Engineering, Av. do Brasil, 101, 1700-066 Lisbon, Portugal
[b] CERIS, DECivil, Instituto Superior Técnico, University of Lisbon, Av. Rovisco Pais, 1049-001 Lisbon, Portugal
[c] cE3c, Centre for Ecology, Evolution and Environmental Changes, Azorean Biodiversity Group, University of Azores, 9700-042 Angra do Heroísmo, Azores, Portugal
[d] iBB, Institute for Bioengineering and Biosciences, Instituto Superior Técnico, University of Lisbon, Av. Rovisco Pais, 1049-001 Lisbon, Portugal
[e] Department of Bioengineering, Instituto Superior Técnico, University of Lisbon, Av. Rovisco Pais, 1049-001 Lisbon, Portugal
[f] CERENA, DECivil, Instituto Superior Técnico, University of Lisbon, Av. Rovisco Pais, 1049-001 Lisbon, Portugal
[g] CERIS, DECivil, NOVA School of Science and Technology, NOVA University of Lisbon, 2829-516 Caparica, Portugal

HIGHLIGHTS

- ETICS were exposed for two years at both urban and maritime environments in Portugal.
- The durability was assessed considering the ETICS condition throughout natural aging.
- The bio-susceptibility and the aesthetic properties after aging were investigated.
- The durability of the complete system was significantly affected by the rendering system formulation.

GRAPHICAL ABSTRACT

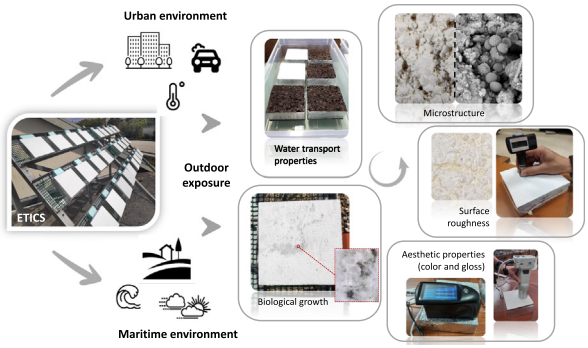

ARTICLE INFO

Editor: Baoliang Chen

Keywords:
ETICS
Durability
Natural aging
Water resistance
Biocolonization
Surface properties

ABSTRACT

External Thermal Insulation Composite Systems (ETICS) are multilayer solutions which provide an enhanced thermal performance to the building envelope. However, significant anomalies can be detected on ETICS facades, in some cases shortly after the application of these systems. This study intends to evaluate and compare the durability of six commercially available ETICS after two years of outdoor exposure at both urban and maritime conditions in Portugal. The systems were characterized by means of non-destructive testing (i.e., visual and microscopic assessment, water transport properties, thermal conductivity, surface roughness), thus allowing to evaluate the performance loss throughout natural aging. The bio-susceptibility and aesthetic properties (color and gloss) were also investigated. Results showed that the performance and durability of the complete system is significantly affected by the rendering system formulation. The lime-based specimens obtained the highest rate of mold development after one year of aging in a maritime environment, becoming considerably darker and with lower surface gloss. Fungal analysis of this darkish stained area indicated the presence of mold species of the genera *Alternaria*, *Didymella*, *Cladosporium* and *Epicoccum*, and yeasts of the genera *Vishniacozyma* and *Cystobasidium*. An increase of both capillary water absorption and water vapor permeability was also registered for the aged lime-based specimens. Acrylic-based systems obtained lower capillary water absorption after aging and greater dirt deposition on their surfaces, especially in urban conditions. These systems had also higher color variation and surface gloss decrease and slightly higher mold growth, when compared with

* Corresponding author at: LNEC, National Laboratory for Civil Engineering, Av. do Brasil, 101, 1700-066 Lisbon, Portugal.
E-mail address: jparracha@lnec.pt (J.L. Parracha).

http://dx.doi.org/10.1016/j.scitotenv.2022.157828
Received 6 May 2022; Received in revised form 7 July 2022; Accepted 31 July 2022
Available online 4 August 2022

those aged in a maritime environment. Finally, no mold growth was detected on the silicate-based specimens after two years of aging. However, these specimens obtained higher capillary water absorption and lower vapor permeability after aging, possibly leading to moisture accumulation within the system. Results contribute towards the development of ETICS with enhanced performance and durability.

1. Introduction

External Thermal Insulation Composite Systems (ETICS) are multilayer solutions which are applied to the building exterior walls, providing an enhanced thermal performance. ETICS generally consist of three layers (the thermal insulation, the base coat, and the finishing coat) with properties optimized with the aim of improving the performance of the entire system (Parracha et al., 2021a).

The application of ETICS significantly increased in Europe over the last decades, in both new and thermal retrofitting of building facades. In fact, the use of ETICS for the thermal retrofitting can lead to a significant reduction of energy losses and gains (Varela Luján et al., 2019). ETICS can also reduce the thermal bridge effect and provide improved indoor thermal comfort due to the increase of thermal inertia (Barreira and de Freitas, 2014). Relatively low implementation costs and easy application, with the possibility of installation without disturbing the residents of the buildings, are among other advantages of these systems. ETICS should also verify a set of requirements related with the hygric behaviour, adhesion to the substrate, resistance to impact, and others (EOTA, 2020) in order to be considered of suitable quality and adequate performance. However, significant anomalies were detected on ETICS facades, in some cases shortly after the application of these systems (Amaro et al., 2013; Kvande et al., 2018). Most of these anomalies are related or can be associated to the presence of water (Maia et al., 2019; Parracha et al., 2020).

Previous studies (Amaro et al., 2013, 2014) showed that biological colonization, color alteration and runoff marks are the most common anomalies on ETICS facades in Portugal. Biological growth, which can be identified in some cases only few years after the construction or thermal retrofit of the building, strongly depends on high levels of surface moisture content, resulting from the combined effect of wind-driven rain, drying process, surface condensation and the rendering properties (Barreira and de Freitas, 2013). According to Gonçalves et al. (2021), ETICS with higher insulation capacity and finished with a white colored surface are generally more prone to biological growth, if compared to systems with lower insulation capacity and a black finishing. In fact, a higher insulation capacity and a white colored surface provide lower values of outdoor surface temperature for a longer time span, and therefore higher risk of surface condensation. Additionally, a slow drying process of the ETICS layers also contributes to an increased risk of biocolonization, as surface moisture content can remain high for long periods. Finally, the use of renders with noticeable amounts of organic additives, which can provide nutrients to microorganisms, can also favor biological growth (Klamer et al., 2004). On this matter, Kvande et al. (2018) pointed out the possibility of biological growth beneath the ETICS due to accumulation of moisture in the building exterior wall, which is particularly relevant in the case of organic-based substrates (e.g., timber). Likewise, the use of organic-based thermal insulation materials can also favor mold growth (Palumbo et al., 2017; Parracha et al., 2021a).

Biological colonization alters the color of the finishing coat and occurs more frequently in areas of high moisture content (i.e., water runoff areas). Shirakawa et al. (2020) evaluated the performance of four different acrylic paints applied on mortar panels after seven years of natural exposure in different Brazilian environments and observed high levels of discoloration and paint detachment in a coastal zone, most probably due to the increased rainfall in this location compared to an urban area. However, paints exposed in an urban environment generally presented higher levels of biocolonization, which were attributed to the higher atmospheric pollution (Shirakawa et al., 2020).

Despite being considered by several authors as aesthetic anomalies, biological colonization, discoloration/color change, and runoff marks can have long-term impact on the thermal and mechanical performance of the ETICS without regular maintenance actions. Nonetheless, aesthetic alteration has a key role in limiting a wider diffusion of ETICS technology.

Some studies have been published on the durability assessment of ETICS (Griciute et al., 2013; Daniotti and Paolini, 2008; Slusarek et al., 2020; Parracha et al., 2021b; Landolfi and Nicolella, 2022), mainly considering accelerated aging cycles simulating the action of different degradation agents (e.g., water, heat, frost, solar or ultraviolet (UV) radiation). However, the synergistic effect of different degradation agents on the long-term durability of ETICS is not easily reproduced in laboratorial conditions, sometimes leading to different degradation mechanisms. Thus, considering the non-linear correlation among accelerated weathering exposure and natural aging, ETICS should also be tested outdoors to understand and confirm their performance.

Landolfi and Nicolella (2022) designed a new accelerated aging method for the evaluation of the long-term durability of ETICS focusing on the role of the thermal insulation, based on the combination of hygrothermal and freeze-and-thaw cycles, that mostly represent European conditions. Results showed an increase of water absorption after aging, whereas the thermal conductivity remained practically unchanged. Slusarek et al. (2020) used hygrothermal and UV accelerated weathering to evaluate the impact of thermal insulation anomalies on the overall performance of ETICS. The authors observed surface cracking and registered an increase of the open porosity of the finishing coat after aging. Furthermore, a study of Griciute et al. (2013) showed higher capillary water absorption after aging for ETICS finished with a silicate-based paint, when compared to ETICS with acrylic-based finishing coats. A different approach based on hygrothermal and UV cycles had been earlier proposed by Daniotti and Paolini (2008) using weather data of Milan, Italy. The authors defined the most important degradation agents to be included in the optimized aging cycles, as well as their frequency and intensity. Nevertheless, the authors also proposed further outdoor exposure of ETICS in order to find a valid correlation among natural exposure and artificial weathering results (Daniotti and Paolini, 2008).

The European guideline EAD 040083-00-0404 (EOTA, 2020) considers only the hygrothermal performance for the durability assessment of ETICS and further degradation agents, such as UV radiation, environmental pollutants and biological colonization are not envisaged in the document. In this context, the identification of the most important degradation agents and the knowledge of the degradation mechanisms and long-term performance of ETICS in different environments are fundamental for a sustainable and efficient use of these systems.

In this study, the durability of six commercially available ETICS was assessed after two years of natural exposure at both urban and maritime zones in Lisbon area, Portugal. The systems were characterized throughout natural aging by means of non-destructive testing (i.e., visual and microscopic assessment, water resistance, thermal conductivity, surface roughness). The bio-susceptibility and aesthetic properties (color and gloss) of the ETICS were also investigated. Moreover, quantification and identification of fungi populations colonizing ETICS surfaces as well as the more favorable conditions for their development were also addressed. By providing a comprehensive insight on the durability of the ETICS considering different exposure conditions (urban vs maritime), a deeper comprehension of the relation between the degradation mechanisms and the synergistic effect of the environmental agents is provided. Results contribute towards the development of ETICS with enhanced performance and durability.

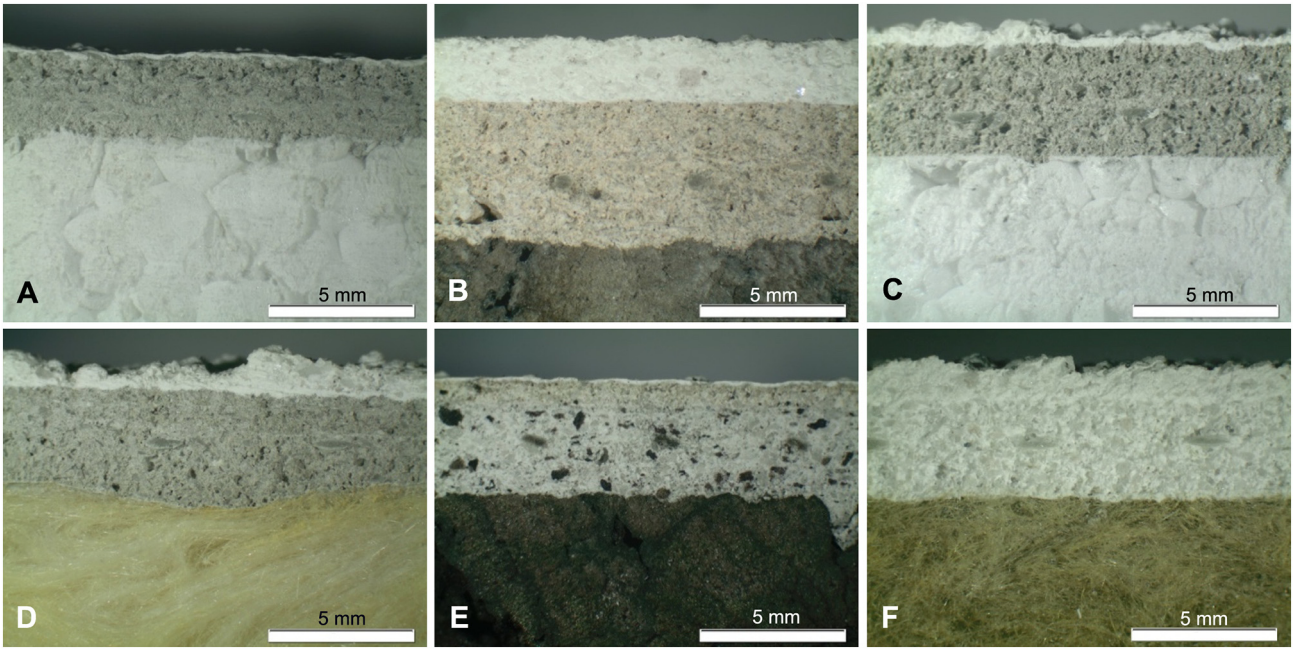

Fig. 1. Cross sections of ETICS E1 (A), E2 (B), E3 (C), E4 (D), E5 (E) and E6 (F) (adapted from Parracha et al., 2021a).

2. Materials and methods

2.1. External thermal insulation composite systems (ETICS)

In a previous study (Parracha et al., 2021b), the durability of six commercially available ETICS was evaluated when exposed to an accelerated aging procedure, comprising a sequence of hygrothermal cycles (heat-rain and heat-cold), UV radiation and exposure to pollutants (SO_2). These same systems, certified with a European Technical Assessment (ETA) following the requirements of the European guideline EAD 040083-00-0404 (EOTA, 2020), were tested in the present work (Fig. 1). The selected ETICS have different thermal insulation material (expanded polystyrene – EPS, expanded cork agglomerate – ICB or mineral wool – MW), base coat (cement or hydraulic lime-based) and finishing coat (acrylic, silicate or lime-based) (Table 1).

2.2. Outdoor natural exposure

Two specimens of each ETICS with dimensions of 150 mm × 150 mm × thickness (Table 1) were placed on the rooftop of a building at the National Laboratory for Civil Engineering (LNEC), nearby Lisbon airport in Portugal (urban area). Two specimens of each ETICS with similar dimensions were also exposed on the rooftop of a building at the NOVA School of Science and Technology (NOVA SST) in Caparica, Portugal (with maritime and semi-rural conditions). The test specimens were waterproofed by sealing with scotch tape and silicone on the four edges and on the backside, placed on a rack tilted 45° facing South and exposed at each of the test sites for two years (Fig. 2), from October 2019 to October 2021. The meteorological conditions for Lisbon and Caparica in the considered timespan, as well as the geographical coordinates of the two natural aging sites, are reported in Table 2.

All specimens were identified based on the system type (Table 1), exposure condition (P – pristine (non-aged), NU – naturally aged at urban zone, NM – naturally aged at maritime zone) and exposure time (O – one year of natural aging, T – two years of natural aging).

2.3. Durability assessment

In order to assess the durability of the different ETICS, a series of laboratory tests were performed on the systems on their pristine conditions and after one and two years of outdoor exposure (Table 3), focusing on the water transport properties, bio-susceptibility and surface properties of the ETICS. Therefore, the samples were collected from the aging sites after one and two years of exposure, tested in laboratorial conditions for approximately one month, and re-exposed. The specimens aged in the maritime environment were not re-exposed after the second-year evaluation,

Table 1
Identification and composition of the ETICS and their components in accordance with the information provided by the manufacturers and available in the ETA document (adapted from Parracha et al., 2021b).

ETICS (E)	Thermal insulation (TI)	Rendering system (RS)		S thickness (TI + RS) [mm]
		Base coat (BC)[a]	Finishing coat (FC)	
E1	EPS	Cement, synthetic resins and mineral additives	Acrylic-based, pigments, marble powder, additives and biocide[b]	36.66 + 3.21
E2	ICB	Natural hydraulic lime, cement, mineral fillers, resins and synthetic fibers	Air lime, hydraulic binder and organic additives	58.83 + 7.02
E3	EPS	Cement, mineral fillers, resins and synthetic fibers	Acrylic-based, mineral aggregates, pigments, additives and biocide[b]	59.99 + 4.54
E4	MW	Cement, mineral fillers, resins and synthetic fibers	Acrylic-based, mineral aggregates, pigments, additives and biocide[b]	56.83 + 4.51
E5	ICB	Natural hydraulic lime, mixed binders and cork aggregates	Silicate-based, organic additives and pigments	38.57 + 5.34
E6	MW	Cement, natural hydraulic lime and aggregates	Acrylic-based, siloxane resin, marble powder and biocide[b]	39.93 + 4.84

Notation:
[a] Includes a glass fiber mesh.
[b] e.g. terbutryn or isothiazole.

Fig. 2. Location of the natural aging sites at LNEC in Lisbon (A) and NOVA SST in Caparica (B) (credits: Google Maps).

Table 2
Geographical coordinates of the natural aging sites and meteorological data for the period of exposure provided by the Portuguese Institute for Sea and Atmosphere (IPMA).

Zone	Geographical coordinates	Exposure period	Maximum mean temperature [°C]	Minimum mean temperature [°C]	Total annual rainfall [mm]	Daily mean solar radiation [kJ/m^2]
Urban	38°45′31″N, 9°08′29″W, Altitude – 95 m	First year	21.7	13.8	559.8	16,768.2
		Second year	21.8	13.0	529.9	17,065.9
Maritime	38°45′36″N, 9°12′25″W, Altitude – 109 m	First year	22.5	9.9	447.0	16,900.9
		Second year	22.2	9.2	510.4	16,689.6

thus allowing to evaluate other properties of the systems (e.g., water vapor permeability, SEM-EDS analysis) that imply the use of smaller samples which were collected from the original specimens.

2.3.1. Visual inspection and stereomicroscope observations

ETICS surfaces were visually inspected each month to detect macroscopically visible anomalies, namely cracking, material loss, or stains. Stereomicroscope observations were performed on the non-aged systems and after one and two years of exposure using a microscope Olympus SZH10 and the Olympus SC30 image acquisition system, with the Olympus LabSens software.

2.3.2. Water absorption by capillarity

The capillary water absorption test was performed in a conditioned room (T = 23 ± 2 °C; RH = 65 ± 5 %) following the EAD 040083-00-0404 guideline (EOTA, 2020). Specimens (Table 3) were previously placed

Table 3
Durability assessment tests performed, sampling and references.

Test	Reference	Sampling [Nr. of specimens × Nr. of systems × Aging condition]	Dimensions [mm]
Visual inspection and stereomicroscope observations	–	2 × 6 × 2	150 × 150 × S thickness
Water absorption by capillarity	EAD 040083-00-0404 (EOTA, 2020)	2 × 6 × 2	150 × 150 × S thickness
Water vapor permeability	EN 1015-19 (CEN, 2008) and EAD 040083-00-0404 (EOTA, 2020)	3[a] × 6 × 1	Cylindrical with ø ~ 70
Thermal conductivity	ASTM D7984 (ASTM, 2016) and EN 1745 (CEN, 2020)	2 × 6 × 2 (3 measurements per specimen)	150 × 150 × S thickness
Gloss and color	ASTM D523-14 (ASTM, 2018) and ASTM D2244 (ASTM, 2015)	2 × 6 × 2 (9 measurements per specimen)	150 × 150 × S thickness
Surface roughness	–	2 × 6 × 2 (9 measurements per specimen)	150 × 150 × S thickness
Bio-susceptibility	ASTM D5590-17 (ASTM, 2017) and ASTM C1338-19 (ASTM, 2019)	2 × 6 × 2	150 × 150 × S thickness

[a] Smaller samples collected from the original specimens; Aging condition = urban or maritime.

for 7 days in the same conditioned room for mass stabilization. The finishing coat layer was then placed in direct contact with the water at a ~3 mm water depth to ensure total submergence. The mass variation due to water absorption was monitored at given time intervals (3 min, 1 h, 4 h, 8 h and 24 h). Both the capillary water absorption coefficient, representing the initial rate of water absorption, and the absorption curves, expressing the mass of absorbed water (kg/m^2) as a function of the square root of time ($min^{0.5}$), were analyzed. The capillary water absorption coefficient (A_w) is obtained by Eq. (1), in which A is the immersed base area (m^2) and M_1 (kg) and M_2 (kg) represent the mass of the specimens at the beginning of the test and after 3 min testing, respectively.

$$A_w = \frac{M_2 - M_1}{A \times \sqrt{3}} \quad (1)$$

2.3.3. Water vapor permeability

Cylindrical specimens with a diameter of ~70 mm were cut from the larger specimens and used for the water vapor permeability (WVP) test (Table 3). WVP was evaluated following the EN 1015-19 (CEN, 2008) and the EAD 040083-00-0404 (EOTA, 2020), adopting the dry cup method. The test was performed in environmental controlled conditions ($T = 23 \pm 2$ °C; RH = 50 ± 5 %) using a desiccant ($CaCl_2$) in order to create a 0 % RH environment inside the cup. Specimens were previously conditioned till mass stabilization and then sealed within a plastic cup using scotch tape and paraffin wax, leaving a gap of air (~20 mm) inside between the desiccant and the thermal insulation layer. The assembled specimens were then placed in the test chamber, forcing the vapor flux to pass through the ETICS layers from the external environment (~50 % RH) to the interior of the cup (~0 % RH). In order to evaluate the rate of water vapor transmission, the specimens were weighed every 24 h till mass stabilization. The water vapor diffusion resistance coefficient (μ) is obtained following Eqs. (2) and (3).

$$\Lambda = \frac{m}{A \times \Delta_p} \quad (2)$$

$$\mu = \frac{1.94 \times 10^{-10}}{\Lambda \times e} \quad (3)$$

In the above equations, Λ is the water vapor permeance, m is the slope of the linear correlation between mass variation and time, A is the area of the specimen, Δ_p is the difference between the interior and the exterior vapor pressure (1403.91 Pa, at 23 °C and 50 % RH, and 0 Pa inside the cup), and e is the thickness of the specimen.

The water vapor permeability was determined for specimens in pristine conditions and after two years of exposure in a maritime environment (see Section 2.3).

2.3.4. Thermal conductivity

The thermal conductivity (λ) was measured on the thermal insulation layer of each system, in accordance with previous studies (Parracha et al., 2021a). Measurements were performed on the thermal insulation layer (i.e., on the backside of the ETICS) using a transient method with an ISOMET 2114 (Applied Precision, Ltd) equipped with a surface probe API 210412 (60 mm diameter). The test was performed following the indications of standards ASTM D7984 (ASTM, 2016) and EN 1745 (CEN, 2020), measuring the thermal conductivity in the dry state (10 °C). Specimens were analyzed in three different spots (Table 3), considering the average values and relative standard deviation obtained for different thermal insulation materials (EPS, ICB and MW) (i.e., λ results for EPS were the average of the λ values obtained for the thermal insulation of the specimens of systems E1 and E3).

2.3.5. Gloss and color

Surface gloss measurements were performed using a specular gloss meter Rhopoint Novo-Gloss Lite, considering a measurement geometry of 60°. Specimens were analyzed in nine different spots using a grid (Table 3). The average values and relative standard deviation were considered.

Color measurements were performed using a Chroma Meter Minolta CR-410 considering the CIELAB color space (L^*, a^*, b^*). The L^* coordinate corresponds to the lightness, ranging between 0 (black) and 100 (white), whereas a^* and b^* are the red/green and yellow/blue coordinates, respectively. Values range from $+a^*$ (red) to $-a^*$ (green) and from $+b^*$ (yellow) to $-b^*$ (blue). The measurements were conducted in specular component included mode (SCI), applying the illuminant D_{65} with an observer angle of 2° and 50 mm diameter area. Specimens were analyzed in nine different spots (Table 3), considering the average values and relative standard deviation. The total color difference (ΔE^*_{ab}) was then calculated using Eq. (4) considering the values of ΔL^*, Δa^* and Δb^*.

$$\Delta E^*_{ab} = \sqrt{(\Delta L^*)^2 + (\Delta a^*)^2 + (\Delta b^*)^2} \quad (4)$$

The color difference is obtained considering the reference color (non-aged specimens) and the color of the specimens after one and two years of exposure (aged specimens).

2.3.6. Surface roughness

Surface roughness was determined using an Elcometer 223 surface profile gauge able to measure the roughness up to 2 mm, with a resolution of 0.001 mm. Specimens were analyzed in nine different spots using a surface grid (Table 3), considering the average values and relative standard deviation.

2.3.7. SEM-EDS analysis

Scanning electron microscopy (SEM) analysis was carried out using both a SEM Hitachi S-2400, working at an acceleration voltage of 20 kV and coupled with an Oxford Inca X-Sight energy dispersive X-ray spectrometer, and a SEM Thermoscientific Phenom ProX G6, working at an acceleration voltage of 15 or 20 kV. Samples were previously sputtered with an Au-Pd (80:20) film.

SEM-EDS analysis was conducted only for samples collected from the non-aged specimens and from those exposed in maritime conditions after two years (see Section 2.3).

2.3.8. Biological colonization

Biological colonization on the surface of the systems was visually assessed using the scale defined in ASTM (2017) for mold development assessment: 0 – no apparent growth (0 % contaminated surface); 1 – traces of growth (<10 % contaminated surface); 2 – light growth (10 to 30 % contaminated surface); 3 – moderate growth (30 to 60 % contaminated surface); and 4 – heavy growth (>60 % contaminated surface). All specimens were visually rated by the same experienced observer by combining visual and stereozoom observations with a stereomicroscope Olympus B061.

2.3.9. Fungal assessment

Whenever a system was rated as 2 (light growth) or more considering the classification scale described in the previous section, samples were collected to enumerate and identify the culturable fungi present in the biocolonization stains. Duplicate samples were collected from the stained area in the specimen surface by swabbing approximately 4 cm^2 with sterile cotton swabs previously soaked in sterile Maximum Recovery Peptone Saline (MRPS) solution supplemented with 0.1 % Tween-20 (Digel et al., 2018). Swab samples were also collected from the surface outside the biocolonization stains (i.e., the whitish areas with no visible color change) for comparison purposes. Each swab head was immediately cut with a sterile scissor and suspended in 1 mL sterile MRPS, followed by 5-min vortexing and 1-h shaking (300 rpm) at room temperature. To obtain fungal colonies, 0.1 mL of the obtained suspensions, and their decimal dilutions, were spread-plated (in duplicate) onto Potato dextrose agar (PDA) medium supplemented with 10 mg/L of chlortetracycline (Ct). All Petri dishes were

incubated at room temperature (20 ± 2 °C) with indirect sun light radiation (simulating natural night/day periods), for 6 days. In addition, each swab head was taken out of the suspension, transferred onto PDA + Ct and incubated during 6 days at the same conditions, to obtain fungi-enriched swabs.

Mold (filamentous fungi) and yeast (unicellular fungi)-like colonies formed on the surface of the spread-plated PDA + Ct were counted for enumeration of colony-forming units (CFU) per swab sample; data reported are average values with standard deviations from duplicate determinations with two independent swabs. In addition, the more prevalent colony types were described based on visible macroscopic characteristics (e.g., colony diameter, pigmentation, shape, margin appearance, texture and elevation). Morphologically distinct mold colonies were sub-cultured onto PDA, and their phylogenetic identification at genus level was performed based on the analysis of the partial sequences of internal transcribed spacer (ITS) regions of the rRNA ribosomal operon. For that, genomic DNA was extracted (Nucleospin soil DNA extraction kit, Mackerey-Nigel) from pure colonies subjected to three liquid nitrogen freezing/thawing cycles. The ITS regions were amplified by PCR (Platinum™ II Hot-Start PCR Master Mix, Invitrogen) with the primers ITS1f and ITS2 (Walters et al., 2015), purified (DNA clean and concentrator-25™ kit, ZymoResearch) and sequenced by an outsourcing service using the Sanger method (GATC Biotech AG, GE). For taxonomic identification, the nucleotide sequences were subjected to BLASTN alignment in the User-friendly Nordic ITS Ectomycorrhiza database (UNITE; Nilsson et al., 2019) and in the "Internal Transcribed Spacer Region (ITS) from Fungi type and reference material" database at the NCBI (National Center for Biotechnology Information). Sequences producing significant alignments with >97 % identity and 0–1 gaps between query and reference sequences were used to infer fungi identification at genus level.

The fungi-enriched swabs were used for the molecular characterization of culturable fungal communities prevalent in the stained area samples. This characterization was based in the phylogenetic analysis of the ITS amplicon sequences obtained from the total DNA extracted from each fungi enriched swab (using the Nucleospin soil DNA extraction kit). The amplicons targeting fungi ITS regions were prepared by PCR as described above and using adequate hybrid primers for ITS1f and ITS2 flanked by Illumina universal primer sequencing for barcode insertion (Karlsson et al., 2020). The purified amplicon mixtures were subjected to Illumina standard procedures of library preparation and MiSeq sequencing at the Instituto Gulbenkian de Ciência (Oeiras, Portugal) Genomic Unit. The QIIME 2 2017.4 was used for the sequence clustering into Operational Taxonomic Units (OTUs) based on a percentage identity with known taxa within specific databases (Bolyen et al., 2019). Raw sequence data were demultiplexed and quality filtered using the q2-demux plugin followed by denoising with DADA2 (Callahan et al., 2016). Taxonomy was assigned to amplicon sequence variants using q2-feature classifier (Bokulich et al., 2018) to classify-sklearn naïve Bayes taxonomy classifier against the UNITE database (version 8.3, dynamic) (Abarenkov et al., 2021).

2.3.10. Statistical analysis

Analysis of variance (ANOVA), followed by the Tukey test, was performed to assess the differences between exposure conditions (non-aged, naturally aged at urban and maritime zones) and exposure time (one and two years of exposure), considering the different measured properties. The software IBM SPSS Statistics V26 was used for the analysis assuming a significance level $p < 0.05$.

3. Results and discussion

3.1. Visual and stereomicroscope observations

Surface condensation was visually detected on the systems (Fig. 3A and Fig. A1 in Supplementary Material) mainly during the early morning periods, regardless of the exposure zone (urban or maritime) and since the beginning of the outdoor exposure. In fact, surface condensation is one of the most frequent causes of anomalies in ETICS, favoring biological colonization (Amaro et al., 2014). Interestingly, stains of possible biological origin were firstly observed on the surface of systems E2 (with ICB thermal insulation and finished with a lime-based mortar) after six months of exposure, being more visible in specimens exposed in maritime conditions (Fig. 3B). It is interesting to note that the surface temperature and surface relative humidity of the systems were monitored from September 2020 to January 2021 in a previous work (Parracha et al., 2021c) and system E2 showed the highest periods of surface condensation, being thus anticipated to be more prone to biological growth (Gonçalves et al., 2021; Dybowska-Józefiak and Wesolowska, 2021).

Stereomicroscope observations performed after one and two years of outdoor exposure confirmed the existence of extensive microcracking on the surface of the ETICS, especially after two years of exposure in both urban and maritime conditions. Microcracking was more frequently observed on the systems presenting higher surface roughness (i.e., the acrylic-based systems E3, E4 and E6), which also presented higher dirt deposition on their surfaces, becoming slightly darker after one-year of exposure (Figs. 3C and A1), if compared to systems with lower surface roughness (i.e., lime-based system E2 or silicate-based system E5). Moreover, dirt deposition was more significant on the ETICS exposed in urban conditions when compared to those exposed in a maritime environment, due to a significantly higher deposited airborne particulate matter associated to various airborne trace pollutants (e.g., unburnt hydrocarbons, SO_2, NO_x, etc.) (Cachada et al., 2019). In fact, the proximity of the urban site to the Lisbon airport and heavy traffic roads (Fig. 2A) makes the systems somewhat more exposed to atmospheric pollutants, thus leading to the formation of stains, that not only alter the ETICS aesthetic appearance, but can also be the cause of further anomalies (Chew and Tan, 2003; Tanaca et al., 2011). Additionally, some surface run-off with occasional loss of paint was detected on the surface of the naturally aged silicate-based systems E5 in both urban and maritime zones.

3.2. Water transport properties

Fig. 4 shows the capillary water absorption curves obtained for each system before and after aging.

Results show that all systems tested on their pristine conditions (non-aged) present a capillary water absorption at 1 h lower than 1 kg/m^2, thus respecting the threshold defined in the European guideline (EOTA, 2020) and in agreement with previous works (Parracha et al., 2021a, 2022). However, this is not the case for the naturally aged systems E2, with ICB thermal insulation and finished with a lime-based mortar (Fig. 4B). In fact, the values of absorbed water obtained for these systems after 1 h testing surpass the 1 kg/m^2 and are slightly higher for the ETICS exposed in urban conditions. Nevertheless, the capillary water absorption results of E2 were rather similar after one or two years of assessment (Fig. 4B).

On the other hand, acrylic-based systems (E1, E3, E4 and E6) obtained lower capillary water absorption after outdoor exposure, when compared to the non-aged systems (Fig. 4A, C, D and F). This trend can be attributed to the combination of leaching, carbonation and dissolution-recrystallization processes of $CaCO_3$ with aging, promoting a reduction of the capillary pores (size between 0.01 and 10 μm), thus improving the compactness and stiffness of the acrylic-based renders (Bochen and Gil, 2009; Griciute and Bliudzius, 2015; Xiong et al., 2021). The formation of $CaCO_3$ crystals (see Section 3.7) can partially obstruct the porous network of the renders, hampering the capillary water absorption (Bochen, 2009; Roncon et al., 2021). It is worth to note that the lower capillary water absorption performance is obtained for the system with EPS TI, cement-based BC and acrylic-based FC (E1), considering both the non-aged and naturally aged conditions (Fig. 4A). In fact, the latter system presents an additional acrylic paint layer with higher FC thickness, when compared to the acrylic-based systems E3 and E4 (Table 1), thus promoting lower capillary water absorption (Sadauskiene et al., 2009; Maia et al., 2018). Additionally, the effect of the thermal insulation material on the capillary water absorption results is also noted. Acrylic-based systems E1 and E6 have similar RS composition and thicknesses

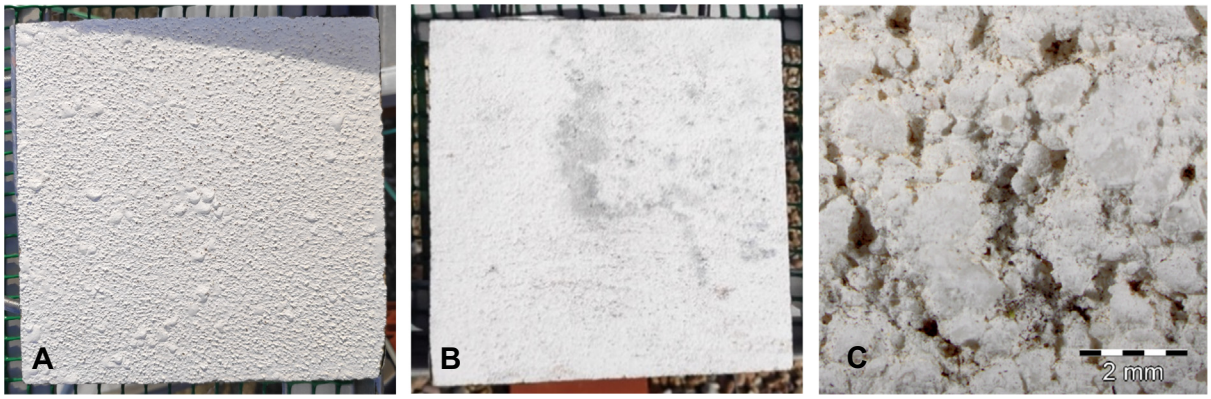

Fig. 3. Surface condensation observed on the silicate-based specimen E5 (A); stains of possible biological origin observed on specimen E2 after one-year of outdoor exposure in a maritime environment (B); dirt deposition detected on the surface of the acrylic-based system E6 after one-year of exposure in an urban environment (C).

(Table 1) and different thermal insulation materials (EPS for E1 and MW for E6). The internal closed pore structure of EPS, when compared to the hydrophilic properties of MW (Gnip et al., 2006; Jerman and Cerný, 2012), promotes a higher capillary water absorption of E6 (Fig. 4A and F).

The water absorption test results obtained for the silicate-based system E5 (Fig. 4E) are slightly higher after natural aging, regardless of the exposure zone (urban or maritime) or time (one or two years). This result may be explained by a partial surface run-off after aging, leading to occasional loss of paint (see Section 3.1). The results obtained are in accordance with those presented by Parracha et al. (2021b) for the same silicate-based system after being subjected to hygrothermal and UV accelerated aging tests.

Fig. 5 shows the results of the capillary water absorption coefficients of the non-aged and naturally aged systems. The highest values were achieved for system E2, which is in line with the results of the capillary absorption curves (Fig. 4B). In fact, system E2 (with ICB TI and lime-based RS) presented the highest values of water absorption and also the highest RS thickness (~7.02 mm) (Table 1). Significantly lower Aw values were obtained for the acrylic-based and silicate-based systems. Acrylic-based system E1, with EPS TI and cement-based BC, presents the lowest Aw both in pristine and aged conditions, showing the best capillary water performance. Similar trends were observed for the other acrylic-based systems (E3 and E4). In this case, results tend to be higher for the non-aged systems and rather similar after natural aging, in accordance with the results of the capillary absorption curves. Although slightly higher, the Aw values of E6 follow a pattern similar to that of E1 (Fig. 5). Finally, the Aw values obtained for the aged silicate-based systems (E5) confirmed a loss of surface hydrophobicity, regardless of the aging condition. This system also presented lower surface hydrophobicity after hygrothermal and UV radiation accelerated tests, while maintaining its hydrophobic features (static contact angle >90°) (Parracha et al., 2021b).

Fig. 6 shows the results of the water vapor diffusion resistance coefficient (μ) of the non-aged and naturally aged (after two years in a maritime environment) specimens (see Section 2.3). The highest μ values were obtained for the acrylic-based systems with EPS as thermal insulation (E1 and E3), whereas the lowest were registered for system E4, with MW TI and an acrylic-based FC. Results highlight the influence of the thermal insulation material choice on the water vapor permeability performance of the whole ETICS. Systems with EPS thermal insulation (E1 and E3) present significantly higher μ values before and after natural aging, when compared to systems with MW or ICB. This trend can be explained by the internal closed pore structure of EPS, presenting a hydrophobic matrix that hinders water penetration in both liquid and vapor phases (Jerman and Cerný, 2012; Cai et al., 2017). However, with the exception of silicate-based system E5 (Fig. 6), all ETICS obtained lower μ values after aging (i.e., higher water vapor permeability), thus decreasing water accumulation within the system and reducing the risk of internal condensation (Mandilaras et al., 2014; Posani et al., 2021).

3.3. Thermal conductivity

The results of the thermal conductivity of the TI of the ETICS after two years of natural aging in urban and maritime environments are shown in Fig. 7. The λ values obtained after two years of aging were not statistically significant different ($p > 0.05$) from those registered in the non-aged state, regardless of the thermal insulation material or exposure condition. A slight increase of the thermal conductivity of EPS (~3.2 %) was obtained after aging in both urban and maritime environments. Despite the higher standard deviation values obtained for the aged TI, the thermal conductivity of ICB remained remarkably close to that of the pristine specimens. Nevertheless, the broad range of standard deviation values obtained after aging (Fig. 7) might indicate a less consistent thermal performance over time (Anh and Pásztory, 2021). Moreover, the largest difference of thermal conductivity (~6.3 %) was obtained for the MW specimens after two years of natural exposure in the urban environment, due possibly to the hydrophilic properties and thus repeated wetting/drying cycles of the MW (Abdou and Budaiwi, 2013).

3.4. Color and gloss

A slight gloss decrease was obtained for all systems after one year of exposure in a maritime environment (Fig. 8). However, results obtained after one-year aging in both urban and maritime environments are not statistically significant different from those obtained before aging ($p = 0.639$ and $p = 0.226$, respectively). In fact, a slight increase is obtained for the lime-based system E2 and for the silicate-based system E5 (Fig. 9) exposed in the urban environment. This increase can be explained by a lower surface roughness of these systems that facilitates surface washing (i.e., caused by wind-driven rain or surface condensation), thus leading to higher values of surface gloss (Ichinose et al., 2009; Parracha et al., 2021a).

On the other hand, significantly lower values of surface gloss were obtained after two years of natural aging in urban and maritime environments ($p < 0.01$), thus indicating coating degradation (Fig. 9). In fact, a gloss variation higher than 0.3 was obtained for all systems, being this value more significant in the case of the acrylic-based system E1, which already presented this trend after one year of exposure in a maritime environment (Fig. 9A). Moreover, surface gloss results obtained after two years of exposure in urban and maritime environments are not statistically significant different among them ($p = 0.769$), indicating a degradation of the coating after two years of aging, regardless of the exposure condition.

Fig. 10 shows the results of the colorimetric coordinates (L*, a*, b*) of the non-aged and naturally aged systems. A significant decrease of lightness (L*) can be observed after one year of aging in both urban and maritime environments ($p < 0.01$). Systems exposed in urban conditions generally gained a considerably darker tone (lower L* values), when compared to systems in maritime conditions ($p < 0.05$). These results can be explained

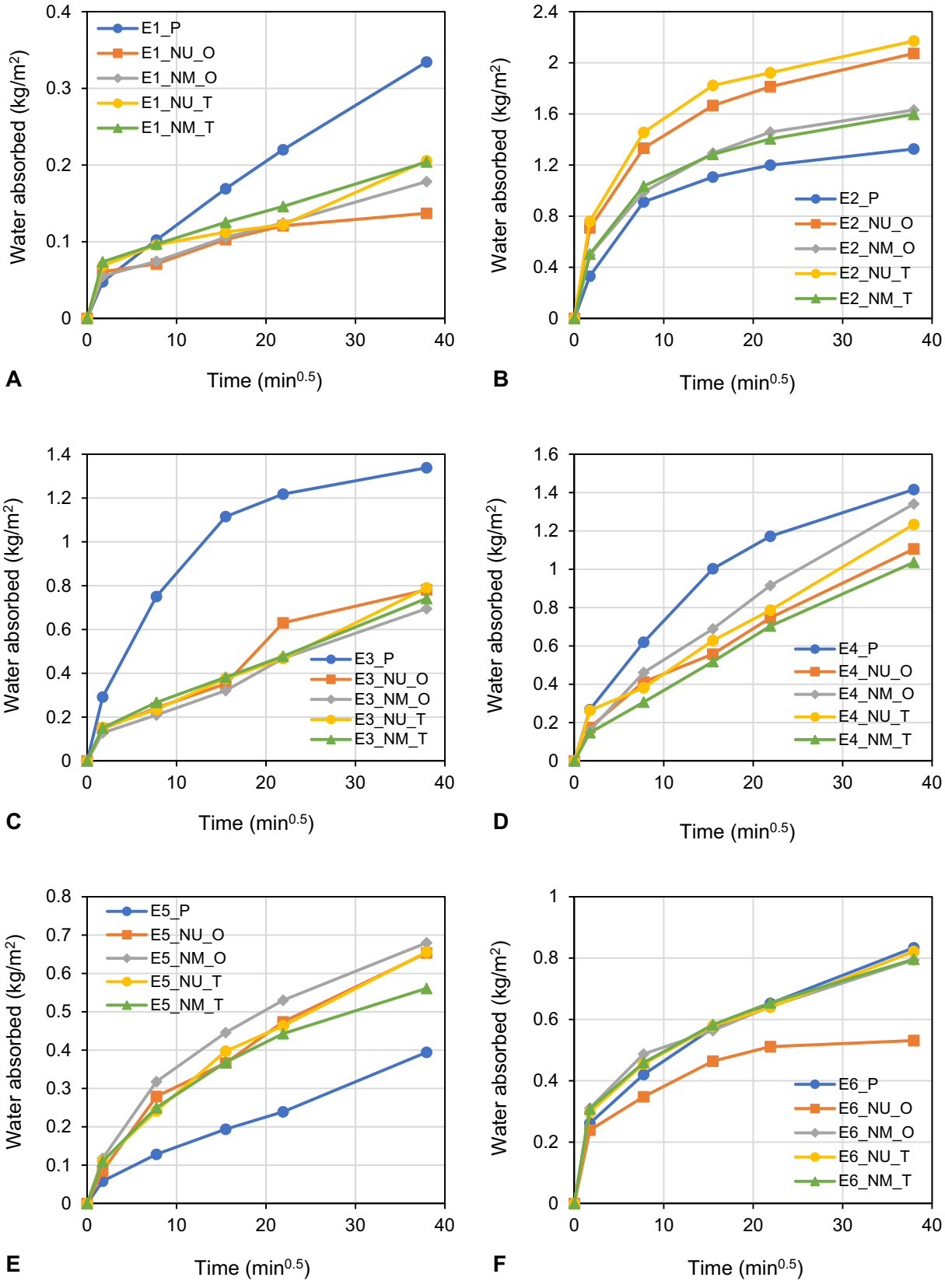

Fig. 4. Capillary absorption curves of non-aged (P) and naturally aged (NU_O, NM_O, NU_T and NM_T) ETICS.

by the deposition of atmospheric particulate matter on the surface of the systems in urban conditions, as previously stated in Section 3.2. Additionally, L* decrease was significantly higher in the acrylic-based systems (E1, E3, E4 and E6) after one year of aging, when compared to the lime-based or silicate-based systems (E2 and E5) (Fig. 10A). On the other hand, significantly lower gloss values were obtained for E1 after two years of natural aging (Figs. 8 and 9), possibly indicating coating degradation (Tilley, 2000), which is also confirmed by a significant L* decrease.

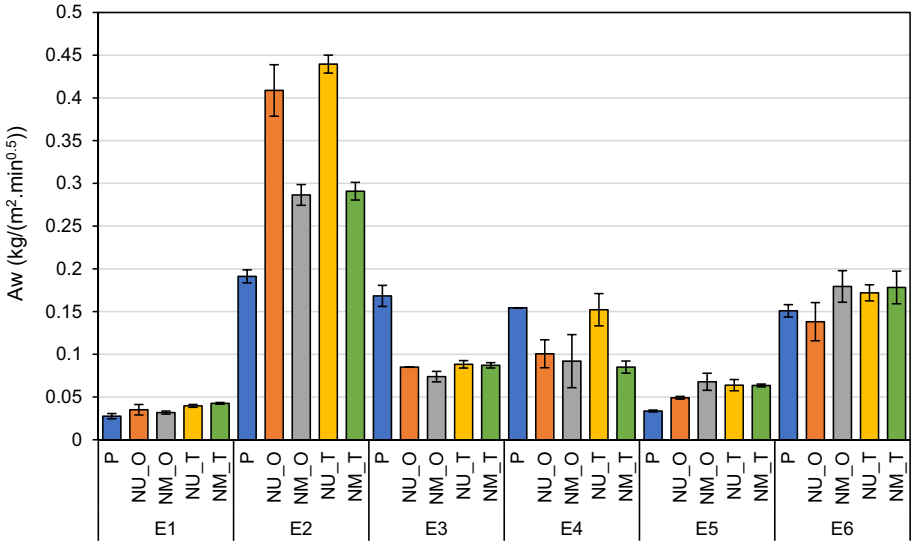

Fig. 5. Results of the capillary water absorption coefficient of non-aged (P) and naturally aged (NU_O, NM_O, NU_T and NM_T) ETICS (average values and relative standard deviation).

The chromatic coordinate a* was significantly more affected after one year of natural aging in urban conditions when compared to maritime conditions ($p < 0.01$). The highest a* increase was obtained for the acrylic-based system E6 (Fig. 10B), with all systems presenting a more reddish tone after aging. However, a* values were not significantly different after two years of aging in urban and maritime environments ($p = 0.543$). This means that the ETICS become significantly more reddish after one year of exposure in an urban zone, followed by a stabilization of that tone after two years of exposure in that environment. On the other hand, this stabilization was not observed for the ETICS exposed in a maritime zone, which gained a considerably more reddish color after two years of aging. The faster aesthetic alteration of the systems in the urban environment can be associated to the higher air pollutants, contributing to an earlier physical degradation of the external surfaces (Diamanti et al., 2015; Shirakawa et al., 2022), if compared to the systems in a maritime environment.

Furthermore, with exception of E2, a significantly higher yellowish coloration was observed in the systems after one year of aging in both urban and maritime environments (Fig. 10C), in accordance with other authors (Paolini et al., 2017; Shirakawa et al., 2020). The highest b* increase in the two exposure zones was obtained for the silicate-based system E5 (Fig. 10C). However, b* values were not significantly different after one or two years of exposure in urban ($p = 0.696$) and maritime ($p = 0.062$) environments, i.e., the highest b* alteration occurred during the first year of exposure. Additionally, a negative variation of b* was obtained only for the system E2, finished with a lime-based mortar. Δb* was higher after two years of natural aging in maritime conditions (Fig. 10C), in accordance with the visual analysis (see Section 3.1). In fact, stains of possible

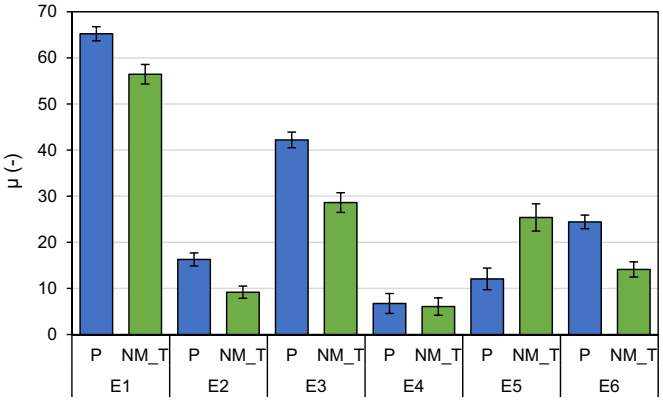

Fig. 6. Results of the water vapor diffusion resistance coefficient of non-aged (P) and naturally aged (NM_T) ETICS (average values and relative standard deviation).

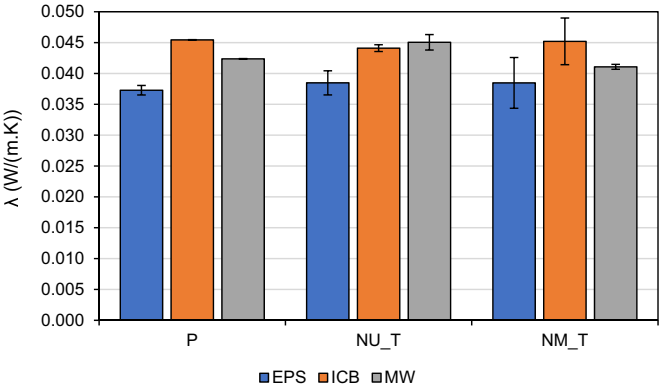

Fig. 7. Results of the thermal conductivity of the non-aged (P) and naturally aged (NU_T and NM_T) insulation materials (average values and relative standard deviation).

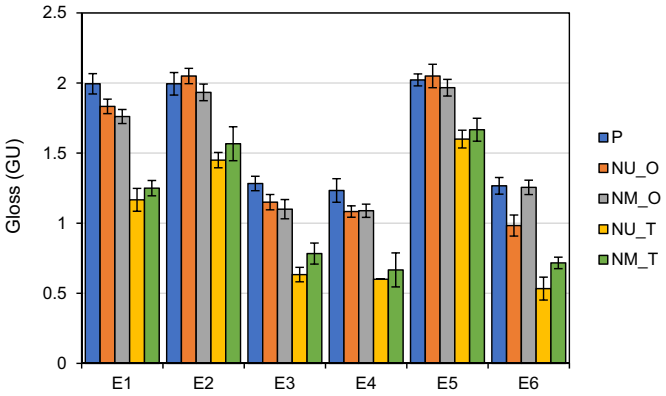

Fig. 8. Results of the specular gloss of non-aged (P) and naturally aged (NU_O, NM_O, NU_T and NM_T) ETICS (average values and relative standard deviation).

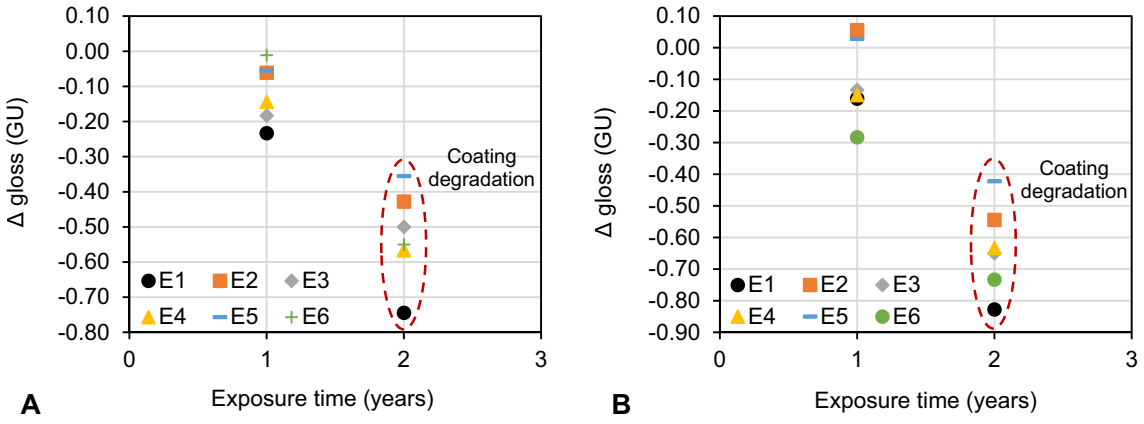

Fig. 9. Average values of gloss variation of ETICS in maritime (A) and urban (B) environments after 1 and 2 years of natural aging.

biological origin were observed on the surface of E2 after one year of outdoor exposure, being more pronounced in the specimens exposed in a maritime environment. In accordance with previous studies (e.g., Shirakawa et al., 2010), a negative variation of b* (i.e., a more bluish coloration) may be associated to biocolonization phenomena.

Finally, a total color variation (ΔE^*_{ab}) > 2 CIELAB units was obtained for all systems after two years of natural aging (Table 4), confirming aesthetic alteration that can be detected by an unexperienced observer (Mokrzycki and Tatol, 2011). The highest values were achieved for the acrylic-based systems E3 and E6 (Table 4).

3.5. Surface roughness

The results of the surface roughness of the non-aged and aged ETICS are presented in Fig. 11. Due to the high dispersion of the results (i.e., high standard deviation especially for systems with a more heterogeneous surface), it was decided to separate the results that were obtained for the non-aged systems (P_U and P_M represent the surface roughness of the non-aged specimens of each system that were subsequently exposed in urban and maritime environments, respectively). It was concluded that P_U and P_M average results are not significantly different ($p = 0.999$).

As shown in Fig. 11, a significant increase of surface roughness ($p = 0.031$) was obtained after one year of aging in an urban environment. Despite being higher, surface roughness results after one year of exposure in a maritime environment were not significantly different from those obtained prior to natural aging ($p = 0.567$), which means that systems exposed in an urban environment were significantly more affected after one year of aging than systems in a maritime environment. In fact, an increase of surface roughness after aging can result from physical-chemical alterations in the coating, thus favoring material loss and film shrinkage (Rashvand and Ranjbar, 2012). Moreover, higher surface roughness can also lead to a greater risk of biocolonization (Barberousse et al., 2007).

After two years of aging, surface roughness decreased for both systems exposed in urban and maritime environments, with rather similar results among the two aging sites. However, no significant changes were obtained after one and two years of natural exposure in urban ($p = 0.09$) and maritime ($p = 0.141$) environments.

3.6. SEM-EDS analysis

SEM-EDS results showed that system E1 (acrylic-based FC) presented initially a homogeneous surface, and that only a limited number of microcracks, lacunas or material loss were observed after two years of natural aging in a maritime environment (Fig. 12A and B), in agreement with the results observed after artificial aging (Parracha et al., 2021b). The other acrylic-based systems (E3, E4 and E6), which had slightly higher surface roughness compared to E1 (Fig. 11), also presented a significant resistance after aging, although a slightly higher degradation, with micro-lacunas and micro-abrasion of the patina (in some spots, some aggregate can be seen) was observed (Fig. 12C and D). These data can support the higher capillary water absorption and water vapor permeability of systems E3, E4 and E6, when compared to E1.

When considering the system E2 with a lime-based FC, the specimens underwent a partial leaching and smoothing of the surface after two years of aging, possibly with processes of dissolution and re-precipitation of $CaCO_3$ (Fig. 12F and G). It is worth noting that no TiO_2 (used both as photocatalytic additive and white pigment) was detected in this specimen (Fig. 12G), and thus no self-cleaning properties are associated to this coating.

The system finished with a silicate-based coating (E5) presented initially a rather homogeneous surface, based on a network of plate-like aggregate of potassium silicate and micro-sized open pores (Fig. 12H). After two years of aging in a maritime environment, a flat surface can still be observed; however, larger plate-like aggregate was reduced to smaller dimension, with some micro-lacunas, and the open pores were partially occluded (Fig. 12I). This coating had a rather high amount of Ti also after aging, which is associated to a partial photocatalytic activity (Fig. 12J).

3.7. Biological colonization

Mold growth results on the finishing coat of the aged ETICS are presented in Table 5. Traces of growth (<10 % of contaminated surface) were firstly observed in the systems after one year of natural aging, except for the silicate-based system E5 and for the acrylic-based systems E4 and E6. The resistance to mold growth of the silicate-based system is noteworthy, which is also in accordance with the results obtained by Parracha et al. (2021b), after exposure to a set of different accelerated aging tests (i.e., hygrothermal cycles, UV radiation, SO_2 exposure) simulating urban environments.

On the other hand, the lime-based system E2 showed the highest rate of biological development after one and two years of aging, regardless of the exposure condition (maritime or urban). Results were slightly higher in the maritime zone, with system E2 presenting light growth (10 to 30 % of contaminated surface) since the first year of exposure (Fig. 13). In fact, system E2 is composed of a cork-based TI material and has cork aggregates as additive in the BC composition. After aging, the surface of this system has higher susceptibility to biological development, due to not only microcracking and surface wear caused by aging, but also to a possible modification of the pore size distribution of the ETICS components, which might have led to an alteration of the water absorption kinetics of the systems (Ravikumar et al., 2012; Kvande et al., 2018) (see Section 3.2). This is especially relevant in the case of renders with substantial amounts of organic additives (Parracha et al., 2021a), as in the case of E2. Therefore, there is a possibility of biological growth in the TI or BC layers due mostly to moisture accumulation, which affects the entire ETICS system and is most noted when the surface is wet (Fig. 13).

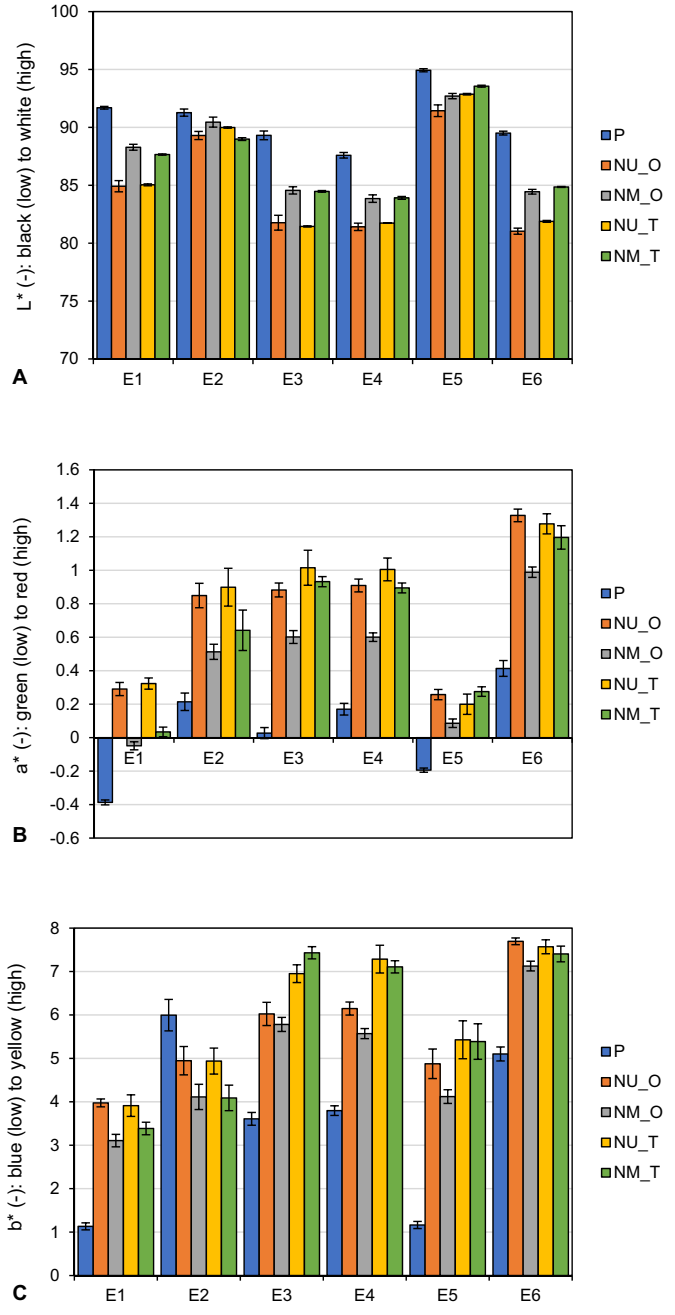

Fig. 10. Results of the CIELAB parameters L* (A), a* (B) and b* (C) of non-aged (P) and naturally aged (NU_O, NM_O, NU_T and NM_T) ETICS (average values and relative standard deviation).

When considering the results obtained for the acrylic-based systems E1 and E3, which present a combination of biocides (terbutryn or isothiazole), it can be observed that mold growth only occurs in the specimens aged in the urban zone after one year of exposure (Table 5). In fact, acrylic-based systems have higher surface roughness (Fig. 11) that facilitates dirt and dust accumulation. According to Tanaca et al. (2011), the deposition of particulate matter on the surface of building materials provides ample nutrients contributing to fungal development.

Table 4
Average values of total color variation of naturally aged ETICS.

	ΔE^*_{ab}			
	NU_O	NM_O	NU_T	NM_T
E1	7.38	3.96	7.25	4.65
E2	2.32	2.08	1.80	3.01
E3	7.97	5.25	8.60	6.23
E4	6.65	4.16	6.87	5.00
E5	5.12	3.71	4.76	4.47
E6	8.91	5.48	8.06	5.25

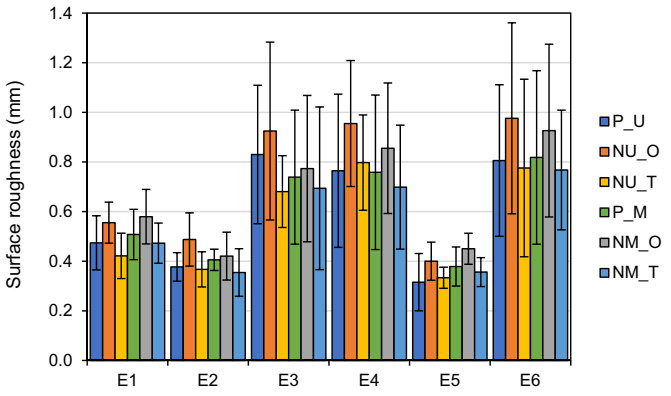

Fig. 11. Results of surface roughness of non-aged (P) and naturally aged (NU_O, NU_T, NM_O and NM_T) ETICS (average values and relative standard deviation).

3.8. Fungi populations in the system E2

As pointed out in the previous section, the lime-based system E2 was rated as 2 (light mold growth) already after one year of outdoor exposure in a maritime environment (Table 5). Therefore, samples were collected from the surface of one specimen E2 to identify the fungi present in the grey-bluish biocolonization stains (Fig. 13). The samples collected within the stained area proved to contain considerable numbers of colony-forming units (CFU) of fungi able to grow in the selective culture medium used, as shown in Fig. 14A. These culturable fungi mainly comprised four different colony-types of molds (filamentous fungi) and two types of yeasts (unicellular fungi), which could be distinguished by their major morphological characteristics, e.g., the mold colonies showed filamentous margins, pulverous to fuzzy surface, and greyish, dry-green, brownish or orange-pinkish colors (Table C1 in Supplementary Material), whereas the yeast-like colonies had smooth surface, entire margin and whitish or pinkish colors (data not shown). Even though fungal colonies could also be found in the samples collected outside the stained area, i.e., in the whitish areas with no visible color change ("out" in Fig. 14A), considerable higher numbers of fungi colonies were found within the grey-bluish stain (about 6-fold) than outside this stained area (Fig. 14A). The phylogenetic identification (at genus level) of the four morphologically different types of mold colonies grown on the spread-plates from the stain samples, indicated they belonged to the genera *Alternaria*, *Cladosporium*, *Didymella* and *Epicoccum* (Table C1). No colonies of the morphological type assigned to the genus *Alternaria* were detected in the spread-plates obtained with the samples collected outside the stained area (Table C1).

In addition, fungal community characterization based on the phylogenetic analysis of the ITS region sequences obtained from the total DNA extracted from the fungi-enriched swabs, indicated the grey-bluish stain to be dominated by OTUs belonging to the mold genera *Alternaria* (29 % relative abundance), *Didymella* (26 %), *Cladosporium* (10 %) and *Epicoccum* (7 %), and yeasts of the genera *Vishniacozyma* (27 %) and *Cystobasidium* (5 %) ("in" in Fig. 14B). On the other hand, outside the stained area, *Didymella*, *Cladosporium* and *Epicoccum* species were also present, but with the yeasts and the *Alternaria* spp. as minor components (<2 %) ("out" in Fig. 14B).

Interestingly, *Alternaria* spp. were highly abundant in the biocolonization stain and appeared to be at very reduced level outside the stained area of E2. The abundant colonizers *Alternaria* spp. and *Cladosporium* spp. are known dark-melanin producing fungi (Pombeiro-Sponchiado et al., 2017), and

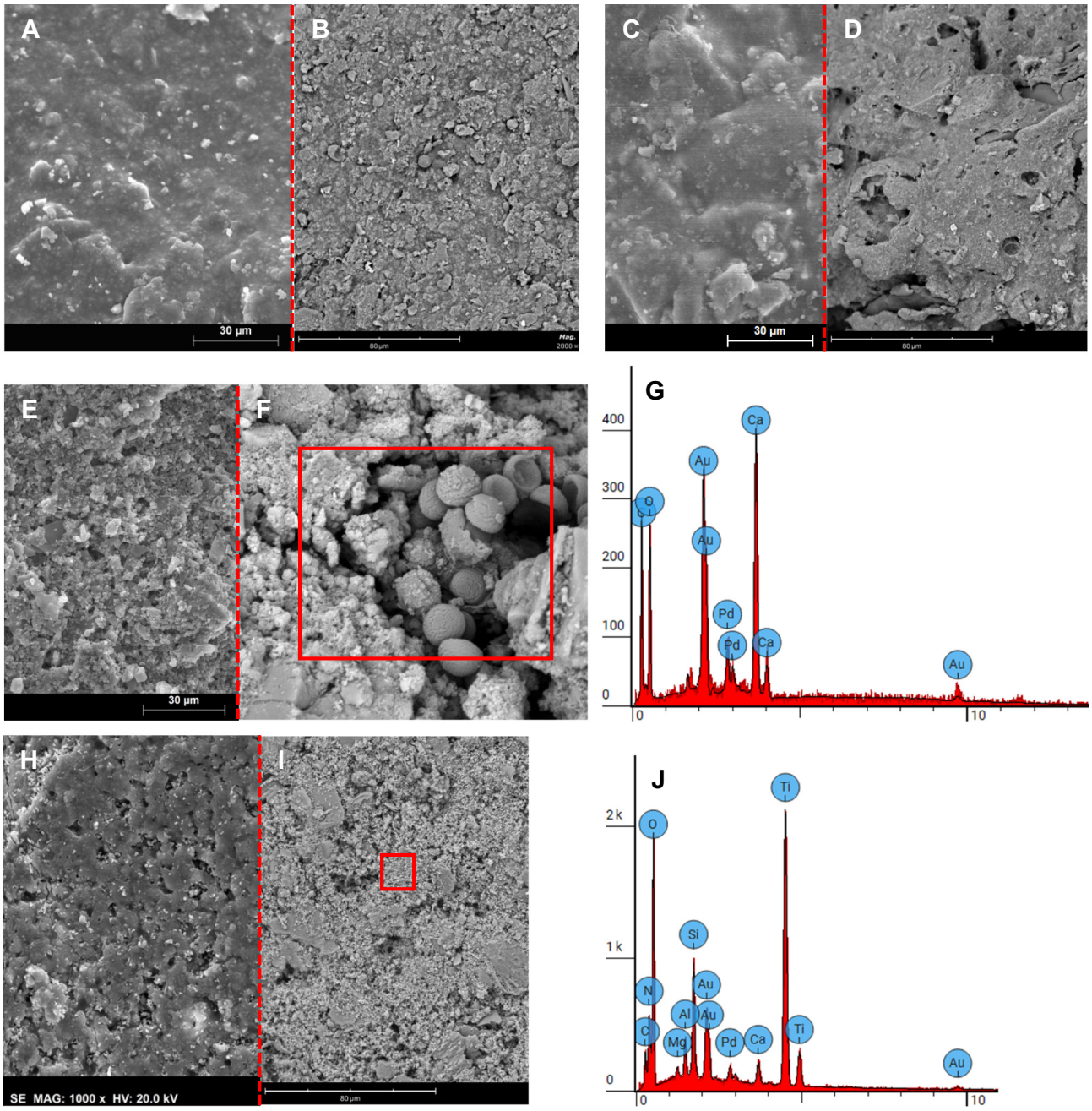

Fig. 12. SEM microphotographs of systems E1 (A, B) and E3 (C, D), both with acrylic-based paints with different mineral charge and thus roughness; system E2 (lime-based finishing) prior (E) and after (F) two years of aging in a maritime environment, and (G) EDS spectrum of (F), where the relevant amount of calcium is attributed to the lime-based finishing coat, and that of carbon possibly also to the presence of biological colonization; system E5 (silicate-based finishing) prior (H) and after (I) two years of aging in the same environment, and (J) EDS spectrum of (I), where an abundance of silica (silicate) and titanium (pigment and/or photocatalytic additive) is identified.

their presence may have contributed for the darkish stain observed in the system E2. However, it should be pointed out that the present microbiological analysis of specimen E2 focused only on fungal populations. The existence of dark stains associated with the presence of certain cyanobacteria species was reported in studies of microbial biofilms formed in different types of building exteriors (Gaylarde and Gaylarde, 2005; Gaylarde et al., 2011) and in natural aging studies of construction materials (Tanaca et al., 2011; Shirakawa et al., 2011) in different environments (Gaylarde and Gaylarde, 2005; Tanaca et al., 2011; Shirakawa et al., 2011). Therefore, the possible presence of other types of microorganisms also able to produce darkish spots, such as several phototrophic species, should not be ruled out.

3.9. Impact of aging on the water transport properties and thermal conductivity of ETICS

It is extensively documented that water is among the most harmful degradation agents of facade coatings, influencing their performance and long-term durability (Pereira et al., 2018). Furthermore, thermal conductivity significantly increases with moisture content (Gomes et al., 2017; Khoukhi et al., 2019), thus leading to an alteration of the thermal performance of the building envelope.

Results showed that non-aged and naturally aged ETICS, except the aged system E2 (finished with a lime-based mortar), had values of 1 h capillary water absorption lower than 1 kg/m^2, thus in accordance with

Table 5
Results of mold growth on the surface of the naturally aged ETICS after 1 and 2 years of aging in urban and maritime environments.

System		Urban environment		Maritime environment	
		One-year	Two-years	One-year	Two-years
E1	1.1	1	1	0	0
	1.2	1	1	0	1
E2	2.1	1	1	2	2
	2.2	1	1	2	2
E3	3.1	1	1	0	0
	3.2	1	1	0	0
E4	4.1	0	0	0	0
	4.2	0	1	0	1
E5	5.1	0	0	0	0
	5.2	0	0	0	0
E6	6.1	0	0	0	0
	6.2	0	1	0	0

the threshold value of EAD guideline (EOTA, 2020). In accordance with previous studies on ETICS with similar composition (Bochen, 2009; Griciute and Bliudzius, 2015; Roncon et al., 2021) a capillary water absorption reduction was observed for the acrylic-based systems (E1, E3, E4 and E6) after aging, possibly due to an alteration of the pore size distribution (Bochen and Gil, 2009; Griciute and Bliudzius, 2015; Xiong et al., 2021). Conversely, a significant hydrophobicity loss occurred for the silicate-based and lime-based systems (E5 and E2, respectively) after natural aging. The capillary water absorption of the lime-based system (E2) was slightly higher in urban conditions, due to microcracking and lacunas (Maia et al., 2019), whereas the homogeneous patina of the silicate-based coatings (system E5) is also affected, with occasional loss of paint. It is worth noting that capillary water absorption results were not significantly different after one or two years of aging in both urban and maritime conditions, meaning that the highest surface degradation for these systems occurred in the first year of exposure.

An increase of the water vapor permeability of the ETICS is observed after two years of aging in a maritime environment, except for the silicate-based system E5. Thus, the significant increase of capillary water absorption obtained after aging for the lime-based system is somehow outweighed by an increase of its water vapor permeability (i.e., the system absorbs more water and also dries faster). The acrylic-based systems (E1, E3, E4 and E6) presented a favorable decrease of capillary water absorption after aging and, at the same time, an increase of water vapor permeability (lower μ). On the other hand, the silicate-based system E5 presented a more unfavorable hygric performance, with higher capillary water absorption after aging, but lower water vapor permeability, possibly leading to

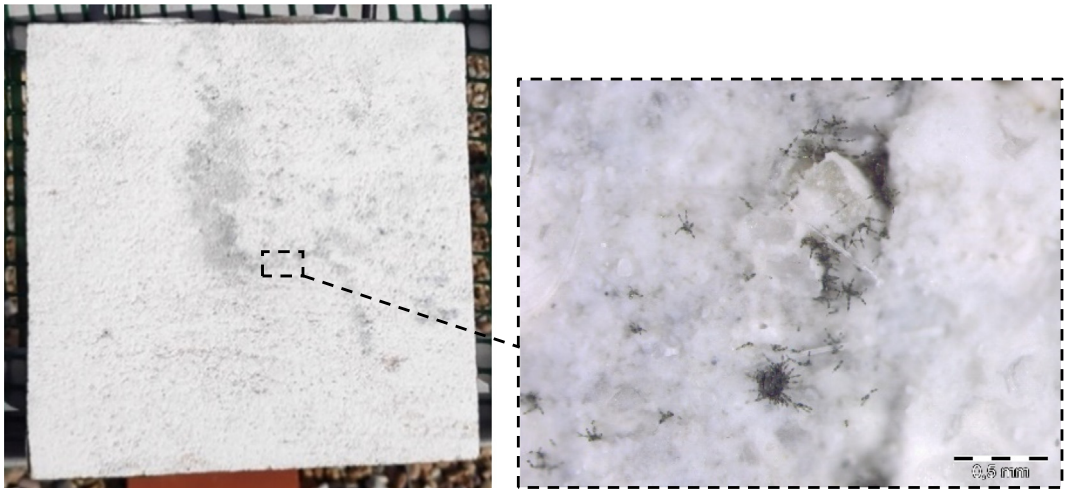

Fig. 13. Mold growth observed on the surface of system E2 after one year of outdoor exposure in a maritime environment.

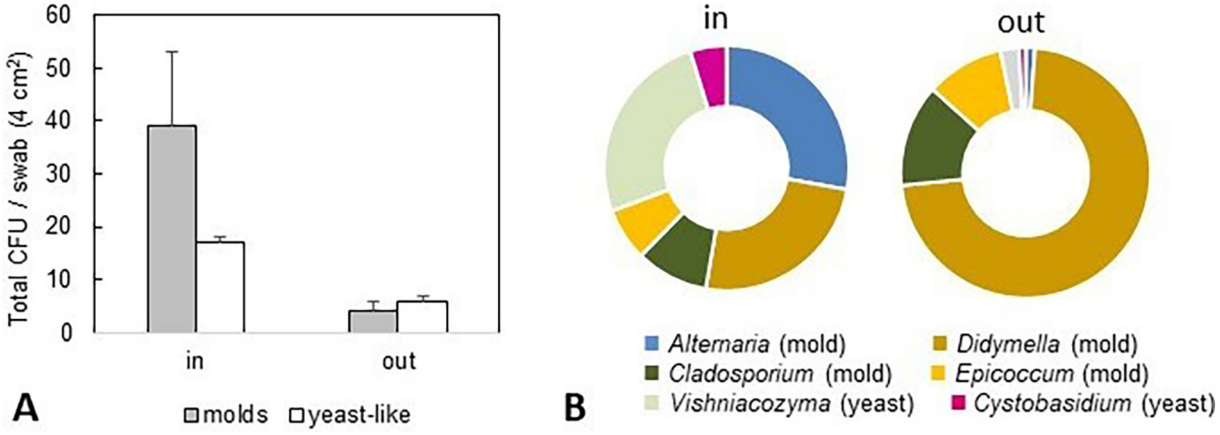

Fig. 14. Fungal assessment of the swab samples collected from the surface of the grey-bluish stain (in) or outside this stained area (out) in one specimen E2 after one year of outdoor exposure in a maritime environment, comprising the number of total colony-forming units (CFU) of fungi (e.g., mold and yeast-like colonies) isolated from the swabs directly by spread-plating in culture medium (A), and the relative abundance of the fungal populations identified, at genus level, in the fungi-enriched swabs (B); for the latter, the relative area of each section in the "donut" representation corresponds to the relative abundance (in %) of Operational Taxonomic Units (OTUs) assigned to the indicated genera, within each sample.

moisture accumulation within the ETICS and favoring further moisture-related anomalies (Kvande et al., 2018; Pereira et al., 2018).

The ETICS thermal conductivity was slightly affected after two years of aging in urban and maritime zones, with the highest thermal conductivity variation (+ 6.3 %) obtained for the hydrophilic mineral wool (MW) after two years in the urban zone, possibly due to the aging of the insulation material (i.e., wetting/drying cycles over time) (Abdou and Budaiwi, 2013; Anh and Pásztory, 2021). A slight increase of λ was obtained for the EPS after aging, whereas results remained almost unchanged for the aged ICB. It can thus be concluded that the thermal conductivity of the ETICS insulation materials was not significantly affected after two years of natural aging, thus confirming the suitable protection provided to the TI by the rendering system of the ETICS.

3.10. Impact of aging on biological colonization and surface properties of ETICS

The highest rate of biological colonization (10 to 30 % of contaminated surface) after one and two years of outdoor exposure was obtained for the lime-based system exposed in the maritime environment. These results can be attributed to several factors, i.e., lack of photocatalytic additive in the finishing coat composition (de Souza and Gaylarde, 2002; Gaylarde et al., 2011); the high capillary water absorption of specimens after aging (Pasanen et al., 2000); and the formation of microcracking and surface wear after aging (Ferrari et al., 2015; Kvande et al., 2018). The incorporation of a biocide on the paint formulation also substantially reduces the risk of biocolonization (de Souza and Gaylarde, 2002). However, some studies showed that surface hydrophobicity and climatic conditions have a more significant role in preventing long-term biocolonization phenomena (Warkentin et al., 2007; Shirakawa et al., 2010). It is worth noting that biological stains are best noted when the surface is wet; thus, the reduced color variation of system E2 after aging can also be justified due to the fact that color measurements were performed in the dry state and in laboratorial conditions. Nevertheless, a decrease in b* chromatic coordinate (i.e., a more bluish coloration) was only obtained for the lime-based system, being this variation higher after two years of aging in maritime conditions. In accordance with previous studies (e.g., Shirakawa et al., 2010), a negative variation of b* CIELAB coordinate may be associated to biological growth. Indeed, the grey-bluish stain formed on the surface of the specimen E2 after one year of aging in a maritime environment proved to be dominated by culturable molds belonging to different genera, namely *Alternaria*, *Cladosporium*, *Didymella* and *Epicoccum*. These fungi are cosmopolitan genera, widely distributed in soil, rocks, vegetation, trees, pollen and dust. For instance, the detected mold genera are among culturable airborne fungal populations recently reported to be found in outdoor air in an urban landscape (Savković et al., 2021), and are some of the most common fungi found on the surface of cementitious building facades (Campana et al., 2020), also affecting stone and external architectural paint films (Gaylarde and Gaylarde, 2005; Gaylarde et al., 2011). Even though the fungal analysis in the present study focused only on system E2, it can be suggested that their distribution in all specimens under study is highly likely, since they were also found in the samples collected from the areas without visible signs of fungal growth, even though with lower numbers than within the grey-bluish stained area. Fungal spores, cells or mycelium fragments can be dispersed in the air and easily reach the ETICS surfaces, where they can find (micro)cracks and organic dirt to which they can attach as well as favorable moisture conditions for germination of spores and cellular growth, thus contributing to a further degradation of the system. Upon growth, these fungi can excrete hydrolytic and oxidative enzymes and produce organic acids, inducing discoloration, cracking, general loss of cohesion and enlargement of crevices, potentially associated with chemical and mechanical anomalies (Ferrari et al., 2015).

Biological growth on the acrylic-based ETICS E1 and E3 only occurred in the urban zone after one year of exposure, which is attributed to the higher atmospheric pollution in Lisbon, and specifically in the urban aging site nearby the airport. Shirakawa et al. (2011) reported similar results, associating the higher fungal colonization in painted mortar surfaces in São Paulo (Brazil) to the higher level of atmospheric pollution, when compared to that in the coastal city of Ubatuba, located in the same state. Additionally, the acrylic-based systems presented the highest surface roughness, thus promoting dirt and dust accumulation which provide ample nutrients and contribute to fungal development in high polluted areas (Guillitte, 1995; Tanaca et al., 2011). The acrylic-based systems exposed in an urban environment had also a higher color variation and surface gloss decrease, in comparison with those aged in a maritime zone. In fact, the formation of biofilms on ETICS surface led to aesthetic alteration, and possibly to further chemical and structural deterioration (English et al., 2003; Gaylarde et al., 2011). Additionally, the acrylic-based systems gained a considerably darker (i.e., lower L* and specular gloss), reddish (i.e., higher a*) and/or yellowish (higher b*) tone, suggesting that aesthetic alteration of the coatings can be related to factors other than biological colonization.

The silicate-based system presented no signs of biological growth after two years of aging at both urban and maritime zones, showing the best performance in this regard. In fact, this finishing coat is based on silica (thus, not being a source of carbon for microorganisms) and has a high alkalinity. Moreover, a further biocide effect is provided by the presence of photocatalytic nanoparticles (TiO_2) in the composition of this coating (Gaylarde et al., 2011; Silva et al., 2022). The silicate-based systems also presented the lowest specular gloss variation after two years of aging in both environments (urban and maritime), as well as one of the lowest values of surface roughness. This latter aspect also contributed to a lower L* (white/dark tone) and a* (green/red tone) variation when compared to the acrylic-based systems. However, a considerable positive variation of b* chromatic coordinate (blue/yellow tone) was registered after aging, with systems presenting a yellowish coloration. The formation of yellow stains on the surface of these systems after hygrothermal artificial aging was also reported by Parracha et al. (2021b).

4. Conclusions

The research aim of this work was to evaluate the durability of different commercially available ETICS when exposed in urban and maritime environments for two years, in order to assess the most significant degradation mechanisms and the related failure modes. The ETICS differ in terms of thermal insulation and rendering system. The following conclusions can be drawn:

- The lime-based system showed the highest rate of biocolonization (10 to 30 % of contaminated surface) from the first year of outdoor exposure in a maritime environment. The aged system also became considerably darker, with a negative variation of b* (a more bluish coloration) and had a significant decrease of surface gloss. Samples from the grey-bluish stained area indicated the presence of the mold genera *Alternaria* (29 %), *Didymella* (26 %), *Cladosporium* (10 %) and *Epicoccum* (7 %), and yeasts of the genera *Vishniacozyma* (27 %) and *Cystobasidium* (5 %). The identification of the fungi colonizing ETICS surfaces is important towards the definition of a suitable maintenance strategy aiming at increasing the long-term durability of the ETICS.
- Acrylic-based systems showed lower capillary water absorption after aging, related to an increase of the compactness and stiffness of the render. These systems presented higher surface roughness and therefore greater dirt deposition on their surfaces, especially in urban conditions. Microcracking was also more frequently observed on these systems, if compared to systems with lower surface roughness (lime-based and silicate-based systems). Moreover, traces of mold growth (<10 % of contaminated surface) were observed on the systems after aging, which were slightly higher in the urban environment. Systems exposed in urban conditions had also higher color variation and surface gloss decrease.

- No mold growth was detected on the silicate-based system after two years of aging, showing the best performance in this regard. In fact, the addition of photocatalytic nanoparticles (TiO_2) can provide improved biocide properties to this coating. These ETICS also presented the lowest gloss variation after aging and lower L* (white/dark tone) and a* (green/red tone) variation when compared to the acrylic-based systems. However, these systems presented a yellowish coloration after aging, with a significant positive variation of b* (blue/yellow tone). Moreover, silicate-based ETICS presented higher capillary water absorption after aging, but lower water vapor permeability, being more prone to moisture accumulation within the system, however without jeopardizing its resistance to mold growth.
- The ETICS thermal conductivity was slightly affected after two years of aging in urban and maritime zones, with the highest thermal conductivity variation (6.3 %) obtained for the hydrophilic mineral wool (MW) after two years in the urban zone. A slight increase of thermal conductivity (3.2 %) was obtained for the EPS after aging, whereas results remained almost unchanged for the aged ICB. It can thus be concluded that the thermal conductivity of the ETICS insulation materials was not significantly affected after two years of natural aging, thus confirming the suitable protection provided to the thermal insulation by the rendering system of the ETICS.

Supplementary data to this article can be found online at https://doi.org/10.1016/j.scitotenv.2022.157828.

CRediT authorship contribution statement

J.L. Parracha: Conceptualization, Methodology, Validation, Formal analysis, Investigation, Writing – original draft, Writing – review & editing, Visualization. **G. Borsoi:** Conceptualization, Methodology, Validation, Formal analysis, Investigation, Writing – original draft, Writing – review & editing, Visualization. **R. Veiga:** Conceptualization, Methodology, Validation, Resources, Writing – review & editing, Funding acquisition. **I. Flores-Colen:** Conceptualization, Methodology, Validation, Resources, Writing – review & editing, Project administration, Funding acquisition. **L. Nunes:** Conceptualization, Methodology, Validation, Resources, Writing – review & editing. **C.A. Viegas:** Conceptualization, Methodology, Validation, Formal analysis, Investigation, Resources, Writing – original draft, Writing – review & editing, Visualization. **L. M. Moreira:** Conceptualization, Methodology, Validation, Formal analysis, Investigation, Resources, Writing – original draft, Visualization. **A. Dionísio:** Conceptualization, Methodology, Validation, Resources, Writing – review & editing. **M. Glória Gomes:** Conceptualization, Methodology, Validation, Resources, Writing – review & editing. **P. Faria:** Conceptualization, Methodology, Validation, Writing – review & editing.

Declaration of competing interest

The authors declare that they have no known competing financial interests or personal relationships that could have appeared to influence the work reported in this paper.

Acknowledgments

The authors acknowledge the Portuguese Foundation for Science and Technology (FCT) for funding the research project PTDC/ECI-EGC/30681/2017 (WGB_Shield – Shielding building facades for cities revitalization. Triple resistance to water, graffiti and biocolonization of external thermal insulation systems), the research units CERIS (UIDB/04625/2020), CERENA (UIDB/04028/2020) and iBB (UIDP/04565/2020), the Associate Laboratory Institute for Health and Bioeconomy – i4HB (LA/P/0140/2020), and the Ph.D. scholarship 2020.05180.BD (J. L. Parracha). The authors also acknowledge CIN, Saint-Gobain and Secil for the material supply and the Portuguese Institute for Sea and Atmosphere (IPMA) for the meteorological data.

References

Abarenkov, K., Zirk, A., Piirmann, T., Pöhönen, R., Ivanov, F., Nilsson, R.H., Kõljalg, U., 2021. UNITE QIIME Release for Fungi. Version 10.05.2021. UNITE Community. https://doi.org/10.15156/BIO/1264708.

Abdou, A., Budaiwi, I., 2013. The variation of thermal conductivity of fibrous insulation materials under different levels of moisture content. Constr. Build. Mater. 43, 533–544. https://doi.org/10.1016/j.conbuildmat.2013.02.058.

Amaro, B., Saraiva, J., de Brito, J., Flores-Colen, I., 2013. Inspection and diagnosis system of ETICS on walls. Constr. Build. Mater. 47, 1257–1267. https://doi.org/10.1016/j.conbuildmat.2013.06.024.

Amaro, B., Saraiva, D., de Brito, J., Flores-Colen, I., 2014. Statistical survey of the pathology, diagnosis and rehabilitation of ETICS on walls. J. Civ. Eng. Manag. 20 (4), 511–526. https://doi.org/10.3846/13923730.2013.801923.

Anh, L.D.H., Pásztory, Z., 2021. An overview of factors influencing thermal conductivity of building insulation materials. J. Build. Eng. 44, 102604. https://doi.org/10.1016/j.jobe.2021.102604.

ASTM, 2015. ASTM D2244, Calculation of Color Tolerances and Color Differences From Instrumentally Measured Color Coordinates. ASTM International, Pennsylvania, USA.

ASTM, 2016. ASTM D7984-16, Standard Test Method for Measurement of Thermal Effusivity of Fabrics Using a Modified Transient Plane Source (MTPS). ASTM International, Pennsylvania, USA.

ASTM, 2017. ASTM D5590-17, Determining the Resistance of Paint Films and Related Coatings to Fungal Defacement by Accelerated Four-week Agar Plate Assay. ASTM International, Pennsylvania, USA.

ASTM, 2018. ASTM D523-14, Standard Test Method for Specular Gloss. ASTM International, Pennsylvania, USA.

ASTM, 2019. ASTM C1338-19, Standard Test Method for Determining Fungi Resistance of Insulation Materials and Facings. ASTM International, Pennsylvania, USA.

Barberousse, H., Ruot, B., Yéprémian, C., Boulon, G., 2007. An assessment of façade coatings against colonisation by aerial algae and cyanobacteria. Build. Environ. 42 (7), 2555–2561. https://doi.org/10.1016/j.buildenv.2006.07.031.

Barreira, E., de Freitas, V.P., 2013. Experimental study of the hygrothermal behaviour of external thermal insulation composite systems (ETICS). Build. Environ. 63, 31–39. https://doi.org/10.1016/j.buildenv.2013.02.001.

Barreira, E., de Freitas, V., 2014. External thermal insulation composite system: critical parameters for surface hygrothermal behaviour. Adv. Mater. Sci. Eng. 650752. https://doi.org/10.1155/2014/650752.

Bochen, J., 2009b. Study of the microstructure of thin-layer facade plasters of thermal insulating system during artificial weathering. Constr. Build. Mater. 23. https://doi.org/10.1016/j.conbuildmat.2009.02.028 2559-1566.

Bochen, J., Gil, S., 2009a. Properties of pore structure of thin-layer external plasters under ageing in simulated environment. Constr. Build. Mater. 23, 2958–2963. https://doi.org/10.1016/j.conbuildmat.2009.02.041.

Bokulich, N.A., Kaehler, B.D., Rideout, J.R., Dillon, M.R., Bolyen, E., Knight, R., et al., 2018. Optimizing taxonomic classification of marker-gene amplicon sequences with QIIME 2's q2-feature-classifier plugin. Microbiome 6, 90. https://doi.org/10.1186/s40168-018-0470-z.

Bolyen, E., Rideout, J.R., Dillon, M.R., Bokulich, N.A., Abnet, C.C., Al-Ghalith, G.A., et al., 2019. Reproducible, interactive, scalable and extensible microbiome data science using QIIME 2. Nat. Biotechnol. 37, 852–857. https://doi.org/10.1038/s41587-019-0209-9.

Cachada, A., Dias, A.C., Reis, A.P., da Silva, E.F., Pereira, R., Duarte, A., Patinha, C., 2019. Multivariate analysis for assessing sources, and potential risks of polycyclic aromatic hydrocarbons in Lisbon urban soils. Minerals 9, 139. https://doi.org/10.3390/min9030139.

Cai, S., Zhang, B., Cremaschi, L., 2017. Review of moisture behavior and thermal performance of polystyrene insulation in building applications. Build. Environ. 123, 50–65. https://doi.org/10.1016/j.buildenv.2017.06.034.

Callahan, B.J., McMurdie, P.J., Rosen, M.J., Han, A.W., Johnson, A.J.A., Holmes, S.P., 2016. DADA2: high-resolution sample inference from Illumina amplicon data. Nat. Methods 13, 581–583. https://doi.org/10.1038/nmeth.3869.

Campana, R., Sabatini, L., Frangipani, E., 2020. Moulds on cementitious building materials – problems, prevention and future perspectives. Appl. Microbiol. Biotechnol. 104, 509–514. https://doi.org/10.1007/s00253-019-10185-7.

CEN, 2008. EN 1015-19, Methods of Test for Mortar for Masonry - Part 19: Determination of Water Vapour Permeability of Hardened Rendering and Plastering Mortars. European Committee for Standardization, Brussels, Belgium.

CEN, 2020. EN 1745, Masonry and Masonry Products. Methods for Determining Thermal Properties. European Committee for Standardization, Brussels, Belgium.

Chew, M.Y.L., Tan, P.P., 2003. Facade staining arising from design features. Constr. Build. Mater. 17 (3), 181–187. https://doi.org/10.1016/S0950-0618(02)00102-2.

Daniotti, B., Paolini, R., 2008. Experimental programme to assess ETICS cladding durability. 11 DBMC International Conference on Durability of Building Materials and Components, pp. 11–14 Istanbul, Turkey.

de Souza, A., Gaylarde, C.C., 2002. Biodeterioration of varnished wood with and without biocide: implications for standard test methods. Int. Biodeterior. Biodegradation 49 (1), 21–25. https://doi.org/10.1016/S0964-8305(01)00102-0.

Diamanti, M.V., Paolini, R., Rossini, M., Aslan, A.B., Zinzi, M., Poli, T., Pedeferri, M.P., 2015. Long term self-cleaning and photocatalytic performance of anatase added mortars exposed to the urban environment. Constr. Build. Mater. 96, 270–278. https://doi.org/10.1016/j.conbuildmat.2015.05.028.

Digel, I., Akimbekov, N.S., Kistaubayeva, A., Zhubanova, A.A., 2018. Microbial sampling from dry surfaces: current challenges and solutions. In: Artmann, G., Artmann, A., Zhubanova, A., Digel, I. (Eds.), Biological, Physical and Technical Basics of Cell Engineering. Springer, Singapore. https://doi.org/10.1007/978-981-10-7904-7_19.

Dybowska-Józefiak, M., Wesolowska, M., 2021. Internal abiotic components that influence the development of biocorrosion on ETICS plasters. Materials 15 (1), 127. https://doi.org/10.3390/ma15010127.

English, S.E., Fjelde, S., Greenhalgh, M., McCabe, R.W., McKenna, T., Morton, L.H.G., Schmidt, B., Sherrington, I., 2003. Laboratory and field studies on thin paint films. Int. Biodeterior. Biodegradation 52, 247–254. https://doi.org/10.1016/S0964-8305(03)00113-6.

EOTA, 2020. EAD 040083-00-0404, Guideline for European Technical Approval of External Thermal Insulation Composite Systems (ETICS) With Rendering. Brussels, Belgium.

Ferrari, C., Santunione, G., Libbra, A., Muscio, A., Sgarbi, E., Siligardi, C., Barozzi, G.S., 2015. Review on the influence of biological deterioration on the surface properties of building materials: organisms, materials, and methods. Int. J. Des. Nat. Ecodyn. 10 (1), 21–39. https://doi.org/10.2495/DNE-V10-N1-21-39.

Gaylarde, C.C., Gaylarde, P.M., 2005. A comparative study of the major microbial biomass of biofilms on exteriors of buildings in Europe and Latin America. Int. Biodeterior. Biodegradation 55, 131–139. https://doi.org/10.1016/j.ibiod.2004.10.001.

Gaylarde, C.C., Morton, L.H.G., Loh, K., Shirakawa, M.A., 2011. Biodeterioration of external architectural paint films – a review. Int. Biodeterior. Biodegradation 65, 1189–1198. https://doi.org/10.1016/j.ibiod.2011.09.005.

Gnip, I.Y., Kerlusis, V., Vejelis, S., Vaitkus, S., 2006. Water absorption of expanded polystyrene boards. Polym. Test. 25 (5), 635–641. https://doi.org/10.1016/j.polymertesting.2006.04.002.

Gomes, M.G., Flores-Colen, I., Manga, L.M., Soares, A., de Brito, J., 2017. The influence of moisture content on the thermal conductivity of external thermal mortars. Constr. Build. Mater. 135, 279–286. https://doi.org/10.1016/j.conbuildmat.2016.12.166.

Gonçalves, M., Simões, N., Serra, C., Almeida, J., Flores-Colen, I., Castro, N.V., Duarte, L., 2021. Onsite monitoring of ETICS comparing different exposure conditions and insulation materials. J. Build. Eng. 42, 103067. https://doi.org/10.1016/j.jobe.2021.103067.

Griciute, G., Bliudzius, R., 2015. Study of the microstructure and water absorption rate changes of exterior thin-layer polymer renders during natural and artificial ageing. Mater. Sci. (Medziagotyra) 21 (1), 149–154. https://doi.org/10.5755/j01.ms.21.1.4869.

Griciute, G., Bliudzius, R., Norvaisiene, R., 2013. The durability test method for external thermal insulation composite system used in cold and wet climate countries. J. Sustain. Archit. Civ. Eng. 1 (2), 50–56. https://doi.org/10.5755/j01.sace.1.2.2778.

Guillitte, O., 1995. Bioreceptivity: a new concept for building ecology studies. Sci. Total Environ. 167, 215–220. https://doi.org/10.1016/0048-9697(95)04582-I.

Ichinose, M., Inoue, T., Sakamoto, Y., 2009. Long-term performance of high-reflectivity exterior panels. Build. Environ. 44, 1601–1608. https://doi.org/10.1016/j.buildenv.2008.10.003.

Jerman, M., Cerný, R., 2012. Effect of moisture content on heat and moisture transport and storage properties of thermal insulation materials. Energy Build. 53, 39–46. https://doi.org/10.1016/j.enbuild.2012.07.002.

Karlsson, E., Johansson, A.-M., Ahlinder, J., Lundkvist, M.J., Singh, N.J., Brodin, T., Forsman, M., Stenberg, P., 2020. Airborne microbial diversity and seasonality in Northern and Southern Sweden. PeerJ. 8, e8424. https://doi.org/10.7717/peerj.8424.

Khoukhi, M., Hassan, A., Saadi, S.A., Abdelbaqi, S., 2019. A dynamic thermal response on thermal conductivity at different temperature and moisture levels of EPS insulation. Case Stud. Therm. Eng. 14, 100481. https://doi.org/10.1016/j.csite.2019.100481.

Klamer, M., Morsing, E., Husemoen, T., 2004. Fungal growth on different insulation materials exposed to different moisture regimes. Int. Biodeterior. Biodegradation 54 (4), 277–282. https://doi.org/10.1016/j.ibiod.2004.03.016.

Kvande, T., Bakken, N., Bergheim, E., Thue, J.V., 2018. Durability of ETICS with rendering in Norway – experimental and field investigations. Buildings 8 (7), 93. https://doi.org/10.3390/buildings8070093.

Landolfi, R., Nicolella, M., 2022. Durability assessment of ETICS: comparative evaluation of different insulating materials. Sustainability 14, 980. https://doi.org/10.3390/su14020980.

Maia, J., Ramos, N.M.M., Veiga, R., 2018. Evaluation of the hygrothermal properties of thermal rendering systems. Build. Environ. 144, 447–449. https://doi.org/10.1016/j.buildenv.2018.08.055.

Maia, J., Ramos, N.M.M., Veiga, R., 2019. Assessment of test methods for the durability of thermal mortars exposure to freezing. Mater. Struct. 52, 112. https://doi.org/10.1617/s11527-019-1411-4.

Mandilaras, I., Atsonios, I., Zannis, G., Founti, M., 2014. Thermal performance of a building envelope incorporating ETICS with vacuum insulation panels and EPS. Energy Build. 85, 654–665. https://doi.org/10.1016/j.enbuild.2014.06.053.

Mokrzycki, W., Tatol, M., 2011. Color difference Delta E-A survey. Mach. Graph. Vision 20, 383–411.

Nilsson, R.H., Larsson, K.-H., Taylor, A.F.S., Bengtsson-Palme, J., Jeppesen, T.S., Schigel, D., Kennedy, P., Picard, K., Glöckner, F.O., Tedersoo, L., Saar, I., Kõljalg, U., Abarenkov, K., 2019. The UNITE database for molecular identification of fungi: handling dark taxa and parallel taxonomic classifications. Nucleic Acids Res. 47, D259–D264. https://doi.org/10.1093/nar/gky1022.

Palumbo, M., Lacasta, A.M., Navarro, A., Giraldo, M.P., Lesar, B., 2017. Improvement of fire reaction and mould growth resistance of a new bio-based thermal insulation material. Constr. Build. Mater. 139, 531–539. https://doi.org/10.1016/j.conbuildmat.2016.11.020.

Paolini, R., Zani, A., Poli, T., Antretter, F., Zinzi, M., 2017. Natural aging of cool walls: impact on solar reflectance, sensitivity to thermal shocks and building energy needs. Energy Build. 153, 287–296. https://doi.org/10.1016/j.enbuild.2017.08.017.

Parracha, J.L., Cortay, A., Borsoi, G., Veiga, R., Nunes, L., 2020. Evaluation of ETICS characteristics that affect surface mould development. DBMC 2020 – XV International Conference on Durability of Building Materials and Components. https://doi.org/10.23967/dbmc.2020.061. 8p, Barcelona, Spain.

Parracha, J.L., Borsoi, G., Flores-Colen, I., Veiga, R., Nunes, L., Dionísio, A., Gomes, M.G., Faria, P., 2021a. Performance parameters of ETICS: correlating water resistance, biosusceptibility and surface properties. Constr. Build. Mater. 272, 121956. https://doi.org/10.1016/j.conbuildmat.2020.121956.

Parracha, J.L., Borsoi, G., Veiga, R., Flores-Colen, I., Nunes, L., Garcia, A.R., Ilharco, L.M., Dionísio, A., Faria, P., 2021b. Effects of hygrothermal, UV and SO2 accelerated ageing on the durability of ETICS in urban environments. Build. Environ. 204, 108151. https://doi.org/10.1016/j.buildenv.2021.108151.

Parracha, J.L., Nunes, L., Gonçalves, F., Pereira, J., Borsoi, G., Flores-Colen, I., Gomes, M.G., Deus, R., Veiga, R., 2021. Mould growth on ETICS: theoretical indices vs in situ observations. CEES 2021 – International Conference – Construction, Energy, Environment & Sustainability. 6p, Coimbra, Portugal.

Parracha, J.L., Borsoi, G., Flores-Colen, I., Veiga, R., Nunes, L., 2022. Impact of natural and artificial ageing on the properties of multilayer external wall thermal insulation systems. Constr. Build. Mater. 317, 125834. https://doi.org/10.1016/j.conbuildmat.2021.125834.

Pasanen, A.-L., Kasanen, J.-P., Rautiala, S., Ikäheimo, M., Rantamäki, J., Kääriäinen, H., Kalliokoski, P., 2000. Fungal growth and survival in building materials under fluctuating moisture and temperature conditions. Int. Biodeterior. Biodegradation 46 (2), 117–127. https://doi.org/10.1016/S0964-8305(00)00093-7.

Pereira, C., de Brito, J., Silvestre, J.D., 2018. Contribution of humidity to the degradation of façade claddings in current buildings. Eng. Fail. Anal. 90, 103–115. https://doi.org/10.1016/j.engfailanal.2018.03.028.

Pombeiro-Sponchiado, S.R., Sousa, G.S., Andrade, J.C.R., Lisboa, H.F., Gonçalves, R.C.R., 2017. Production of melanin pigments by fungi and its biotechnological applications. In: Blumenberg, M. (Ed.), Melanin. IntechOpen, pp. 47–75. https://doi.org/10.5772/67375.

Posani, M., Veiga, M.R., de Freitas, V.P., 2021. Towards resilience and sustainability for historic buildings: a review of envelope retrofit possibilities and a discussion on hygric compatibility of thermal insulations. Int. J. Archit. Herit. 15 (5), 807–823. https://doi.org/10.1080/15583058.2019.1650133.

Rashvand, M., Ranjbar, Z., 2012. Degradation and stabilization of an aromatic polyurethane coating during an artificial aging test via FTIR spectroscopy. Mater. Corros. 65 (1), 76–81. https://doi.org/10.1002/maco.201206544.

Ravikumar, H.R., Rao, S.S., Karigar, C.S., 2012. Biodegradation of paints: a current status. Indian J. Sci. Technol. 5 (1), 1–11. https://doi.org/10.17485/ijst/2012/v5i1.33.

Roncon, R., Borsoi, G., Parracha, J.L., Flores-Colen, I., Veiga, R., Nunes, L., 2021. Impact of water-repellent products on the moisture transport properties and mould susceptibility of external thermal insulation composite systems. Coatings 11, 554. https://doi.org/10.3390/coatings11050554.

Sadauskiene, J., Stankevicius, V., Bliudzius, R., Gailius, A., 2009. The impact of the exterior painted thin-layer render's water vapour and liquid water permeability on the moisture state of the wall insulating system. Constr. Build. Mater. 23 (8), 2788–2794. https://doi.org/10.1016/j.conbuildmat.2009.03.010.

Savković, Ž., Stupar, M., Unković, N., Ivanović, Ž., Blagojević, J., Popović, S., Vukojević, J., Grbić, M.L., 2021. Diversity and seasonal dynamics of culturable airborne fungi in a cultural heritage conservation facility. Int. Biodeterior. Biodegradation 157, 105163. https://doi.org/10.1016/j.ibiod.2020.105163.

Shirakawa, M.A., Tavares, R.G., Gaylarde, C.C., Taqueda, M.E.S., Loh, K., John, V.M., 2010. Climate as the most important factor determining anti-fungal biocide performance in paint films. Sci. Total Environ. 408, 5878–5886. https://doi.org/10.1016/j.scitotenv.2010.07.084.

Shirakawa, M.A., Loh, K., John, V.M., Silva, M.E.S., Gaylarde, C.C., 2011. Biodeterioration of painted mortar surfaces in tropical urban and coastal situations: comparison of four paint formulations. Int. Biodeterior. Biodegradation 65, 669–674. https://doi.org/10.1016/j.ibiod.2011.03.004.

Shirakawa, M.A., de Lima, L.N., Gaylarde, C.C., Silva Junior, J.A., Loz, P.H.F., John, V.M., 2020. Effects of natural aging on the properties of a cool surface in different Brazilian environments. Energy Build. 221, 110031. https://doi.org/10.1016/j.enbuild.2020.110031.

Shirakawa, M.A., de Lima, L.N., Gaylarde, C., Fernandes-Hachich, V., Junior, J.A.S., John, V.M., 2022. The influence of environment and carbonation of fiber cement tiles on the reflectance of a cool surface exposed in four Brazilian cities. Energy Build. 245, 111550. https://doi.org/10.1016/j.enbuild.2021.111550.

Silva, A.S., Borsoi, G., Parracha, J.L., Flores-Colen, I., Veiga, R., Faria, P., Dionísio, A., 2022. Evaluating the effectiveness of self-cleaning products applied on external thermal insulation composite systems (ETICS). J. Coat. Technol. Res. https://doi.org/10.1007/s11998-022-00617-x.

Slusarek, J., Orlik-Kozdón, B., Bochen, J., Muzyczuk, T., 2020. Impact of the imperfection of thermal insulation on structural changes of thin-layer façade claddings in ETICS. J. Build. Eng. 32, 101487. https://doi.org/10.1016/j.jobe.2020.101487.

Tanaca, H.K., Dias, C.M.R., Gaylarde, C.C., John, V.M., Shirakawa, M.A., 2011. Discoloration and fungal growth on three fiber cement formulations exposed in urban, rural and coastal zones. Build. Environ. 46, 324–330. https://doi.org/10.1016/j.buildenv.2010.07.025.

Tilley, R., 2000. Colour and the Optical Properties of Materials. Wiley, Chichester, England.

Varela Luján, S., Viñas Arrebola, C., Rodríguez Sánchez, A., Aguirela Benito, P., González Cortina, M., 2019. Experimental comparative study of the thermal performance of the façade of a building refurbished using ETICS. Sustain. Cities Soc. 51, 101713. https://doi.org/10.1016/j.scs.2019.101713.

Walters, W., Hyde, E.R., Berg-Lyons, D., Ackermann, G., Humphrey, G., Parada, A., Gilbert, J.A., Jansson, J.K., Caporaso, J.G., Fuhrman, J.A., Apprill, A., Knight, R., 2015. Improved bacterial 16S rRNA gene (V4 and V4-5) and fungal internal transcribed spacer marker gene primers for microbial community surveys. mSystems 1, e00009-15. https://doi.org/10.1128/mSystems.00009-15.

Warkentin, M., Schumann, R., Messal, C., 2007. Faster evaluation. Eur. Coat. J. 9, 26–28 30, 32.

Xiong, H., Yuan, K., Xu, J., Wen, M., 2021. Pore structure, adsorption, and water absorption of expanded perlite mortar in external thermal insulation composite system during aging. Cem. Concr. Compos. 116, 103900. https://doi.org/10.1016/j.cemconcomp.2020.103900.